## AD NUMBER

**ADB261475**

## NEW LIMITATION CHANGE

TO

**Approved for public release, distribution unlimited**

FROM

**Distribution authorized to U.S. Gov't. agencies only; Proprietary Info.; Jan 2000. Other requests shall be referred to US Army Medical Research and Materiel Comd., Fort Detrick, MD 21702-5012.**

## AUTHORITY

**USAMRMC ltr, 26 Nov 2002**

AD_____

Award Number: DAMD17-99-1-9010

TITLE: Angiostatic Therapy: A New Treatment Modality for Prostate Cancer

PRINCIPAL INVESTIGATOR: Per Borgstrom, Ph.D.

CONTRACTING ORGANIZATION: Sidney Kimmel Cancer Center
San Diego, California 92126

REPORT DATE: January 2000

TYPE OF REPORT: Annual

PREPARED FOR: U.S. Army Medical Research and Materiel Command
Fort Detrick, Maryland 21702-5012

# NOTICE

USING GOVERNMENT DRAWINGS, SPECIFICATIONS, OR OTHER DATA INCLUDED IN THIS DOCUMENT FOR ANY PURPOSE OTHER THAN GOVERNMENT PROCUREMENT DOES NOT IN ANY WAY OBLIGATE THE U.S. GOVERNMENT. THE FACT THAT THE GOVERNMENT FORMULATED OR SUPPLIED THE DRAWINGS, SPECIFICATIONS, OR OTHER DATA DOES NOT LICENSE THE HOLDER OR ANY OTHER PERSON OR CORPORATION; OR CONVEY ANY RIGHTS OR PERMISSION TO MANUFACTURE, USE, OR SELL ANY PATENTED INVENTION THAT MAY RELATE TO THEM.

## LIMITED RIGHTS LEGEND

Award Number: DAMD17-99-1-9010
Organization: Sidney Kimmel Cancer Center
Location of Limited Rights Data (Pages):

Those portions of the technical data contained in this report marked as limited rights data shall not, without the written permission of the above contractor, be (a) released or disclosed outside the government, (b) used by the Government for manufacture or, in the case of computer software documentation, for preparing the same or similar computer software, or (c) used by a party other than the Government, except that the Government may release or disclose technical data to persons outside the Government, or permit the use of technical data by such persons, if (i) such release, disclosure, or use is necessary for emergency repair or overhaul or (ii) is a release or disclosure of technical data (other than detailed manufacturing or process data) to, or use of such data by, a foreign government that is in the interest of the Government and is required for evaluational or informational purposes, provided in either case that such release, disclosure or use is made subject to a prohibition that the person to whom the data is released or disclosed may not further use, release or disclose such data, and the contractor or subcontractor or subcontractor asserting the restriction is notified of such release, disclosure or use. This legend, together with the indications of the portions of this data which are subject to such limitations, shall be included on any reproduction hereof which includes any part of the portions subject to such limitations.

THIS TECHNICAL REPORT HAS BEEN REVIEWED AND IS APPROVED FOR PUBLICATION.

Nancy Marcus Mabra
12/22/00

_____

_____

_____

# REPORT DOCUMENTATION PAGE

Form Approved
OMB No. 074-0188



| 1. AGENCY USE ONLY (Leave blank) | 2. REPORT DATE | 3. REPORT TYPE AND DATES COVERED |
|---|---|---|
| | January 2000 | Annual (1 Jan 99 - 31 Dec 99) |

**4. TITLE AND SUBTITLE**
Angiostatic Therapy: A New Treatment Modality for Prostate Cancer

**5. FUNDING NUMBERS**
DAMD17-99-1-9010

**6. AUTHOR(S)**
Per Borgstrom, Ph.D.

**7. PERFORMING ORGANIZATION NAME(S) AND ADDRESS(ES)**
Sidney Kimmel Cancer Center

San Diego, CA 92121
E-MAIL: pborgstrom@skcc.org

**8. PERFORMING ORGANIZATION REPORT NUMBER**

**9. SPONSORING / MONITORING AGENCY NAME(S) AND ADDRESS(ES)**
U.S. Army Medical Research and Materiel Command
Fort Detrick, Maryland 21702-5012

**10. SPONSORING / MONITORING AGENCY REPORT NUMBER**

**11. SUPPLEMENTARY NOTES**
This report contains colored photos

**12a. DISTRIBUTION / AVAILABILITY STATEMENT**
Distribution authorized to U.S. Government agencies only (proprietary information, Jan 00). Other requests for this document shall be referred to U.S. Army Medical Research and Materiel Command, 504 Scott Street, Fort Detrick, Maryland 21702-5012.

**12b. DISTRIBUTION CODE**

**13. ABSTRACT** *(Maximum 200 Words)*

The overall goal is to investigate if blockade of vascular endothelial growth factor in combination with conventional cytotoxic agents could be a new innovative treatment regimen for hormone-refractory prostate cancer. We proposed to use our in vivo model to examine the capacity of a soluble VEGF receptor fusion protein (flt-IgG) to inhibit angiogenesis and growth of tumor tissue derived from patients and compare with established prostate cancer cell lines. We experienced very poor growth of prostate carcinoma implanted in our in vivo system, however, since the stroma plays a pivotal role in prostate cancer progression, we hypothesized that the model would be much improved if we were to develop a more "orthotopic milieu". To achieve this goal, we implanted murine prostate tissue prior to implantation of tumor spheroids. Interestingly, adult prostate tissue becomes highly re-vascularized. However, the murine stroma did not much affect growth of human biopsies, but, growth of the murine prostate carcinoma cell line TRAMP C2, was significantly enhanced. We hypothesized, that the "stromal factors" are species specific. We therefore isolated peritumor fibroblasts from one of our biopsies and mixed these with the tumor cells, which resulted in significantly higher growth rates. We had proposed to label tumor cells with an in vivo dye (CMTMR), but due to serious limitations with the in vivo dye, we introduced a histone-GFP fusion protein as a marker for our tumor cells. This labeling technique allows us to evaluate not only tumor size, but also mitotic and apoptotic indices of the implanted tumor spheroids. With these significant and necessary modifications we have a unique pseudo-orthotopic model, which allows us to evaluate, in prostate cancer, in detail the underlying mechanisms behind chemotherapy and angiostatic mediated tumor regression.

| 14. SUBJECT TERMS | 15. NUMBER OF PAGES |
|---|---|
| Prostate | 36 |
| | 16. PRICE CODE |

| 17. SECURITY CLASSIFICATION OF REPORT | 18. SECURITY CLASSIFICATION OF THIS PAGE | 19. SECURITY CLASSIFICATION OF ABSTRACT | 20. LIMITATION OF ABSTRACT |
|---|---|---|---|
| Unclassified | Unclassified | Unclassified | Limited |

## FOREWORD

Opinions, interpretations, conclusions and recommendations are those of the author and are not necessarily endorsed by the U.S. Army.

___ Where copyrighted material is quoted, permission has been obtained to use such material.

___ Where material from documents designated for limited distribution is quoted, permission has been obtained to use the material.

___ Citations of commercial organizations and trade names in this report do not constitute an official Department of Army endorsement or approval of the products or services of these organizations.

X In conducting research using animals, the investigator(s) adhered to the "Guide for the Care and Use of Laboratory Animals," prepared by the Committee on Care and use of Laboratory Animals of the Institute of Laboratory Resources, national Research Council (NIH Publication No. 86-23, Revised 1985).

N/A For the protection of human subjects, the investigator(s) adhered to policies of applicable Federal Law 45 CFR 46.

N/A In conducting research utilizing recombinant DNA technology, the investigator(s) adhered to current guidelines promulgated by the National Institutes of Health.

N/A In the conduct of research utilizing recombinant DNA, the investigator(s) adhered to the NIH Guidelines for Research Involving Recombinant DNA Molecules.

N/A In the conduct of research involving hazardous organisms, the investigator(s) adhered to the CDC-NIH Guide for Biosafety in Microbiological and Biomedical Laboratories.

PI - Signature 1/28/00 Date

## TABLE OF CONTENTS

## INTRODUCTION

The overall goal of this project is to investigate if blockade of vascular endothelial growth factor in combination with conventional cytotoxic agents could be a **new innovative treatment regimen** for hormone-refractory prostate cancer. The original proposal had to specific aims: 1) Evaluate the angiogenic potential of three different human prostate cancer cell lines as well as of tumors obtained directly from surgical samples, and evaluate the efficacy of a neutralizing VEGF-antibody to inhibit their angiogenesis and growth, using our *in vivo* model designed for quantitative studies of the microvascular changes associated with the implantation of small human tumor spheroids in skinfold chambers of nude mice (Fig. 1), and 2) Evaluate combination treatments, combining the anti-VEGF antibody with Estramustine phosphate and Etoposide to assess effective curative strategies for metastatic prostate cancer.

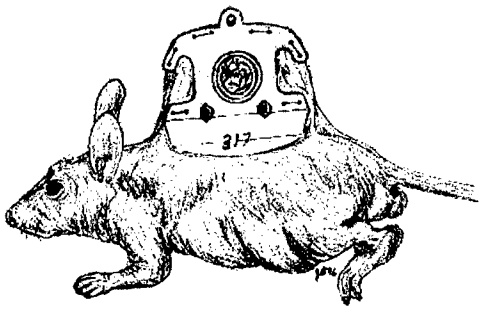

**Figure 1. Cartoon demonstrating the dorsal skinfold technique ih nude mice`**

During the period January 1 to April 1 1999, we worked towards the first specific aim, i.e., to evaluate angiogenic activity of some human prostate cancer cell lines, and the ability of an anti-VEGF moAb, to block their angiogenesis.

In the original application we had proposed to label the tumor cells with an in vivo dye (CMTMR). This technique however had serious limitations in that the labeling lasts at most for 2 – 3 weeks, where-after it becomes very difficult to assess tumor size. Also, we experienced difficulties to distinguish between live CMTMR labeled tumor cells and macrophages that had engulfed the tumor cells.

In the last few years, green fluorescent protein (GFP) has become one of the most widely used tools in molecular and cell biology. The fact that GFP can generate an internal highly visible fluorophore has made it a tremendously valuable in vivo marker. The development of GFP localized to the nucleus (1) has made GFP labeling even more valuable, in that it allows visualization of chromosome dynamics directly in vivo. We thus decided to implement this technique to our system. To accomplish this, a retroviral H2B-GFP vector was constructed.

A Histone-H2B-GFP fusion protein vector construct provided from Dr Wahl at the Salk institute was subcloned into a LXRN vector using the available KpnI and NotI sites. This retroviral vector was transfected along with a VSVG envelope construct into GP-293 cells. Viral supernatants harvested after 72 hours were concentrated at 50,000xg to generate high titer retroviral stocks for transducing prostate carcinoma tissues and cell lines. Cells can be optionally selected for drug resistance in G418 following transduction *in vitro*. We have to date transduced DU145, three PC3 variants with different metastatic capacity, and two LNCAP variants. We have also established collaboration with Dr. Sawyers at UCLA, who has kindly provided one of his early human prostate carcinoma cell lines (LAPC 4) (2). The LAPC 4 is an androgen sensitive prostate cell line derived from a primary tumor.

Finally, we have introduced in our system, a murine prostate cell line TRAMP C2, which was derived from transgenic adenocarcinoma mouse prostate. (3). The introducton of a syngeneic model, we feel is very important, since this allows us also to use this model in immunotherapy studies. The LAPC 4 and the TRAMP C2, both have been transduced with H2B-GFP.


**Figure 2 Photomicrographs illustrating the usefulness of H2B-GFP, in determining tumor size (A, B), and to assess mitotic and apoptotic indices (C) C shows a dividing cell, and E, and F mitotic catastrophy and apoptotic nuclea respectively..**

The value of this labeling technique can not be over emphasized. Not only does it allow us to evaluate tumor size with very high accuracy, but also, it allow us to assess mitotic and apoptotic indices of the implanted tumor cells. Under high magnification, the underlying mechanisms behind chemotherapy and angio-static mediated tumor regression such as cell cycle arrest, mitotic catastrophe, or apoptosis can be distinguished. Temporal and spatial relation of vessel density to cell death allows detailed quantitative evaluation of regimen effectiveness. We believe that the ability of our system to continuously assess apoptotic indices is of great importance to clarify the mechanisms underlying the anticancer effect of the combination of estramustine and taxol. Figure 2 illustrates the usefulness of H2B-GFP transfected cells. The H2B-GFP has been shown not to affect cell cycle progression in vitro (1), however, after implantation of tumor spheroids obtained from cells transfected with the H2B-GFP fusion protein, we detected very high apoptotic indices, especially with the LNCAP cell line which has wild type p53. This was a severe set-back, but we finally managed to resolve this issue. Localization of GFP to the nucleus, made the transfected cells very light sensitive. Once diagnosed, the cure was quite simple, the cover slips were covered with black electric tape. With covered cover slips apoptotic indices decreased significantly. However, even with decreased apoptotic indices, we still had very low mitotic indices.

It is well documented that the stroma plays a pivotal role in prostate cancer progression. Prostatic development occurs via mesenchymal-epithelial interactions in which urogenital sinus mesenchyme induces epithelial morphogenesis, regulating epithelial proliferation and evoking the expression of epithelial androgen receptors and prostate-specific secretory proteins (4, 5). The presence of a stromal androgen receptor is required for this effect (4), and humoral factors, such as keratinocyte growth factor have been shown to be mediated in stromal epithelial paracrine fashion. The adult prostate is also under control of multiple steroid hormone and paracrine peptide factors, and there is evidence that the prostatic stroma plays a major role in

mediation of androgen effects on prostatic epithelium. Thus, prostatic stromal cells are critically involved in growth and progression of prostate cancer. Hence it is not surprising that a marginally tumorigenic cell line such as LNCaP cells acquires much higher tumorigenic and metastatic potential after orthotopic implantation into the prostate (6). Also hormone independent cell lines (DU 145, PC3) become much more tumorigenic and acquire a higher rate of lymph node metastasis after orthotopic rather than after subcutaneous implantation (6).

In the dorsal skinfold chamber, the prostate stroma of course is absent, and in an effort to develop a more "orthotopic milieu" for the prostate carcinoma cells in the chamber, we decided to try and implant pieces of mouse prostate from a donor mouse into the chambers.

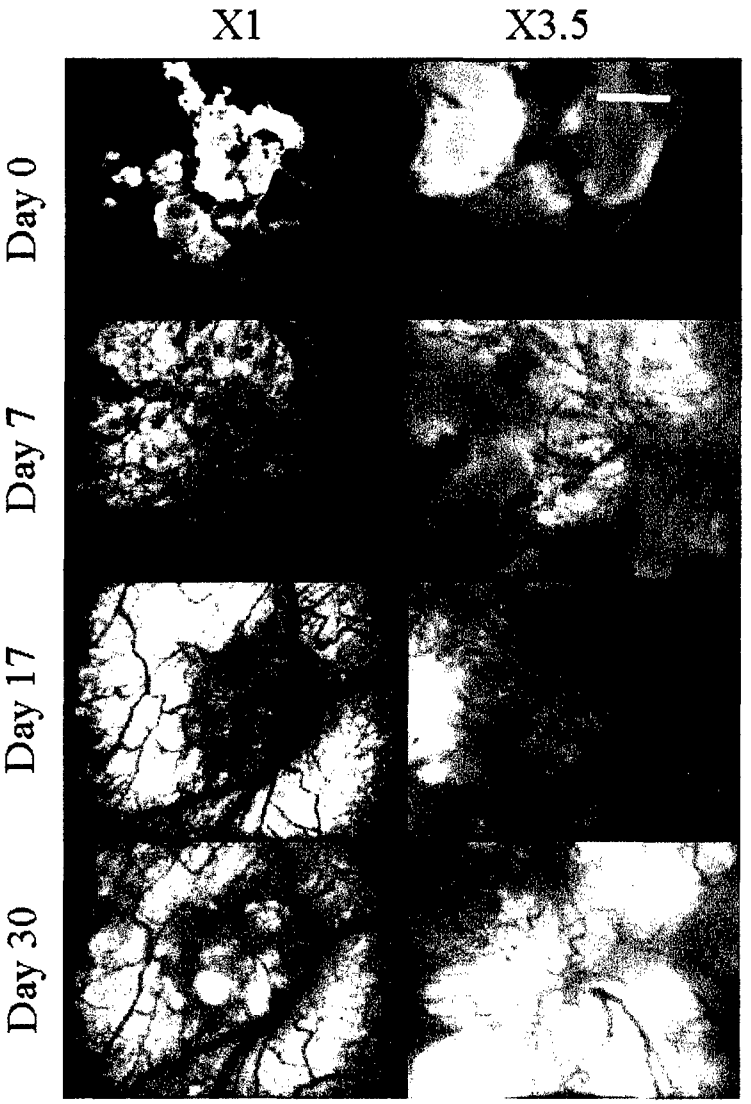


**Figure 3 illustrates the effects of transplantation of adult prostate into dorsal skinfold chambers in nude mice. The prostate pieces were labeled with a rhodamine based in vivo dye (CMTMR), allowing us to track the implanted prostate cells. White bar equals 1.5 mm in left panels and**

Interestingly, also adult prostate implanted in dorsal skinfold chambers evoked a dramatic angiogenic response, and 10-14 days after implantation the tissue was fully re-vascularized and prostatic secretions could be visualized within the reformed ducts (Fig. 3). The fact that adult prostate induces re-vascularization makes it a unique tissue. No other adult tissues we have attempted to implant in the chamber, induces angiogenesis. To date we have tried lung, kidney, mammary fat pads, and skin, non of which evoked any response. Thus, we have successfully managed to re-establish normal adult murine prostate tissue into dorsal skinfold chambers of nude mice. We hypothesized that the introduction of the stroma would greatly improve growth in our in vivo system. This was true for the murine prostate carcinoma cell line TRAMP C2 the mitotic index of which increased dramatically when implanted in chambers primed with prostate tissue. However we noticed no major differences for human cell lines implanted with or without prostate tissue, and hypothesized that "factors" released from the stroma were species specific. In an attempt to introduce

human prostatic "stroma factors", we cultured human fibroblasts obtained from a thin needle biopsy from a patient with diagnosed prostate carcinoma. Tumor spheroids were then made from a 50/50 mixture of tumor cells and the human prostatic peri-tumoral fibroblasts. The introduction of human fibroblasts resulted in significant increases in mitotic indices, as illustrated in Figure 4.

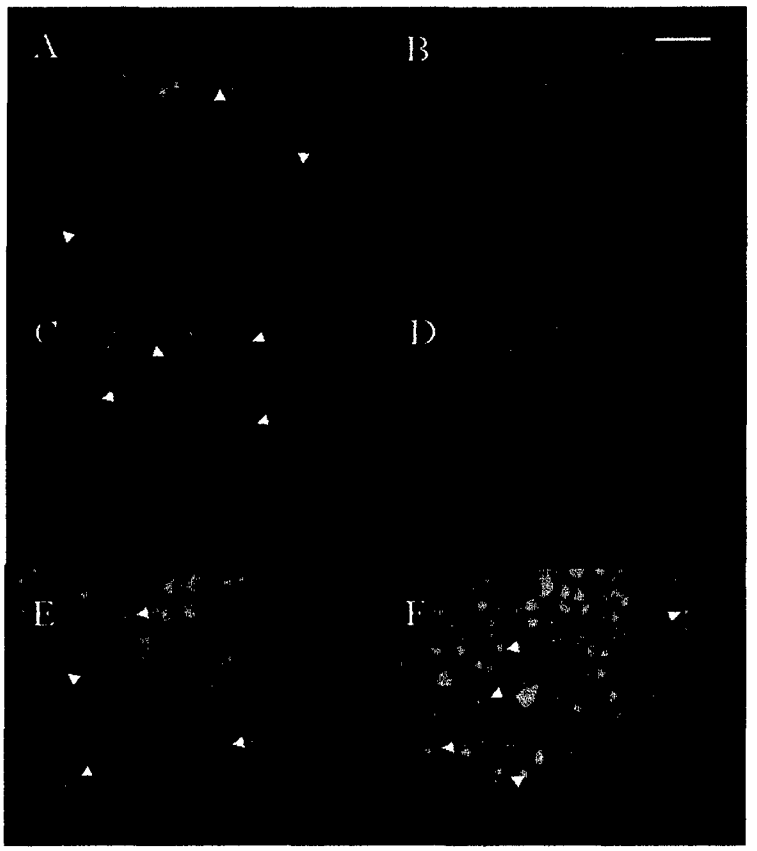


**Figure 4 Photomicrographs obtained from dorsal skinfold chamber implanted with a 50/50 mix of prostate fibroblasts and DU 145 cells transduced with H2B-GFP (A, C). Fibroblasts are labeled with a rhodamine based dye (CMTMR), (B, and D). White bar equals 85 μm. Panels E and F were obtained from tumor spheroids obtained from only DU145 cells. Arrows in A and C illustrate mitotic plates, and arrows in E and F illustrate apoptotic cells.**

In April 1999, negotiations were entered into to eliminate scientific overlap in this project as a result of an additional award made by NCI. The revised Statement of Work was accepted on July 14, 1999 and work towards the revised aims resumed. Please note that all work on the project was temporarily stopped during the negotiation period of April 1 through July 14, 1999,

The revised aims are: 1) Evaluate the angiogenic potential of tumor tissues derived from human prostate cancer thin needle biopsies and compare with established prostate cancer cell lines. Examine the capacity of a soluble VEGF receptor fusion protein (flt-IgG) to inhibit their angiogenesis and growth, using our *in vivo* model designed for quantitative studies of the microvascular changes associated with the implantation of micro tumors, and 2) Evaluate combination treatments, combining the flt-IgG with Estramustine phosphate and Taxol to assess effective curative strategies for prostate cancer biopsies xenografts.

We are presently setting up production of the soluble VEGF receptor IgG chimera (flt-IgG) in quantities sufficient for the proposed series of experiments. Whole murine IgG constant light chain was fused to the carboxy-terminus of the extracellular domain of murine flt and cloned into PCDNA3. This flt-IgG chain was electoporated into SP2/0 non secreting myeloma line and clones tested by ELISA with anti mouse constant IgG (Pharmingen, San Diego). The high producing clone will be grown in spinner culture and purified using the monoclonal anti-Ig constant mAb and eluted with glycine. The purified flt-IgG will be tested for inhibition of VEGF function first in the chamber model using local administration followed by systemic administration i.p.

We will also attempt to achieve VEGF blockade by means of systemic gene therapy, and are in the process of constructing an adenoviral vector for the soluble VEGF receptor flt. Two different flt constructs have been generated for use in the anti angiogenesis models. The first is the naturally occuring murine soluble VEGF receptor variant (sflt), which we have successfully cloned from adult lung and kidney cDNA from C57Bl/6 organs. This sflt is a naturally occurring variant that lacks the transmembrane domain due to intron retention and a stop codon with this intron. This construct has been subcloned into an adenoviral shuttle vector for recombination and transduction either directly in the chamber or into circulation for production by the liver. In addition, we have generated a murine sflt mouse IgG constant light chain chimera which will allow us to purify large quantities of sflt-IgG using an anti mouse IgG light chain monoclonal antibody. As a means to provide VEGF blockade, we had proposed to use the flt-IgG, however, we have also started a collaboration with Sugen Inc, South San Francisco, who will provide us with their selective VEGF TK inhibitor (SU5416), as well as their new inhibitor SU6668, which inhibits VEGF, bFGF, and PDGF. Studies are underway using the TRAMP C2 model to evaluate combination treatment regimens combining the TK inhibitors with Estramustine and Taxol. As mentioned above the use of this syngeneic sustem, allows us also to study immune therapy in combination with angiostatic and conventional chemotherpy.

Regarding thin needle biopsies from patients with prostate tumors, so far we have processed 15 biopsies, however 10 of these were found to be benign prostate hypertrophy (BPH). Currently, after we receive the specimens, they are cultured in PBEM (Clonetics, San Diego CA) without hydrocortisone, until the proper diagnosis has been established. In the event that we have a malignant prostate carcinoma, the biopsies are implanted in a dorsal skinfold chambers. However, we have experienced very slow growth, and currently are investigating the possibilities to implant the biopsies in chambers with established murine prostate as well as with cultured peri-tumoral prostate fibroblasts. For evaluation of growth of the biopsies, we have used the in vivo dye CMTMR, however due to it's limitations, we are presently also attempting to transduce the tumor cells in situ with our retroviral H2B-GFP vector,

**KEY RESERCH ACCOMPLISHMENTS**

- Construction of retroviral H2B-GFP vector
- Establishing stable H2B-GFP clones of the following cell lines; DU145, three variants of PC3, two variants of LnCAP, LAPC 4, and TRAMP C2
- Development of "pseudo-orthotopic" in vivo model to study angiogenesis and growth of micro tumors of prostate carcinoma implanted in nude mice.
- Generation of two different flt constructs for use in the proposed research.

**REPORTABLE OUTCOMES**

None to report at this time.

**CONCLUSIONS**

Though, we did experience a number of setbacks implementing prostate cell lines to our in vivo system, these setbacks have now all been resolved. We now have a unique pseudo-ortotopic in vivo model, which allow us to evaluate in detail, the underlying mechanisms behind chemotherapy and angiostatic mediated tumor regression such as cell cycle arrest, mitotic catastrophe, or apoptosis in prostate carcinoma. Using the H2b-GFP retroviral systems to label tumor cell populations, and the development of flt-IgG and sflt gene therapy constructs, we are now well prepared

to examine the potential synergy of angiostatic therapies with and without standard chemotherapy regimens. We strongly feel that the use of human prostate stromal cells, as well as normal murine prostate tissue transplanted into the drosal skinfold chamber is a unique model by which to study prostate tumor growth. Prostate carcinoma cells, which are notoriously difficult to propagate in murine models and are heavily dependent upon stromal factors, have been enhanced for their tumorigenic potential by providing this orthotopic milleiu of both human and murine stromal compnents. We believe that this system is superior to the current orthotopic xenograft protocols, in that tumors now can be observed in the orthoptopic environment without the need for constant histologic preparations and serial sectioning of the sacrificed animals at different time points. Moreover, the critical mechanism based questions underlying tumor regression under combinatorial therapies, are now well within our reach.

## REFERENCES


1. Kanda T; Sullivan KF; Wahl GM. Histone-GFP fusion protein enables sensitive analysis of chromosome dynamics in living mammalian cells. Curr Biol, 1998 Mar, 8:7, 377-85

2. Klein KA; Reiter RE; Redula J; Moradi H; Zhu XL; Brothman AR; Lamb DJ; Marcelli M; Belldegrun A; Witte ON; Sawyers CL. Progression of metastatic human prostate cancer to androgen independence in immunodeficient SCID mice. Nat Med, 1997 Apr, 3:4, 402-8

3. Foster BA; Gingrich JR; Kwon ED; Madias C; Greenberg NM. Characterization of prostatic epithelial cell lines derived from transgenic adenocarcinoma of the mouse prostate (TRAMP) model. Cancer Res, 1997, 57:16, 3325-30.

4. Condon MS ; Bosland MC. The role of stromal cells in prostate cancer development and progression. In Vivo; 13(1):61-5 1999.

5. Cunha GR. Role of mesenchymal-epithelial interactions in normal and abnormal development of the mammary gland and prostate. Cancer; 74(3 Suppl):1030-44 1994.

6. Rembrink K ; Romijn JC ; van der Kwast TH ; Rubben H ; Schroder FH.Orthotopic implantation of human prostate cancer cell lines: a clinically relevant animal model for metastatic prostate cancer. Prostate; 31(3):168-74 1997.

## APPENDIX CONTENTS

ANTICANCER RESEARCH *19*: 4203-4214 (1999)

# Importance of VEGF for Breast Cancer Angiogenesis *in Vivo*: Implications from Intravital Microscopy of Combination Treatments with an Anti-VEGF Neutralizing Monoclonal Antibody and Doxorubicin*

PER BORGSTRÖM[1,3], DANIEL P. GOLD[3], KENNETH J. HILLAN[2] and NAPOLEONE FERRARA[2]

[1]*La Jolla Institute for Experimental Medicine 11077 North Torrey Pines Road, La Jolla, CA 92037;*
[2]*Genentech Inc. 460 Point San Bruno Boulevard, South San Francisco CA 94080,*
*and* [3]*Sidney Kimmel Cancer Center, 10835 Altman Row, San Diego, CA 92121, U.S.A.*

**Abstract.** *In the present study, we evaluated the effects of a neutralizing anti-Vascular Endothelial Growth Factor (VEGF) mAb, A4.6.1(200 μg twice weekly, i.p.), on angiogenesis and growth of tumor spheroids of human breast cancer cell lines (MCF-7, ZR-75 and, SK-BR-3) in nude mice. Furthermore, we investigated if in the presence of effective VEGF blockade, a conventional chemotherapeutic drug (doxorubicin, (5 mg/kg, weekly) could be effective, and if so would there be an additive effect of the combination regimen. Tumor Spheroids were implanted in dorsal skinfold chambers in nude mice. Tumor cells were pre-labeled with a fluorescent vital dye (CMTMR), which allowed the estimation of growth of implanted tumor spheroids. FITC (fluorescein isothiocyanate)-Dextran was used to evaluate formation of neo-vasculature at the tumor site. In control animals all three cell-lines produced extensive neovasculature and there was significant tumor growth throughout the observation period. Treatment with the anti-VEGF mAb caused significant suppression of angiogenic activity for all cell lines, stressing the critical role VEGF plays in breast tumor angiogenesis. Doxorubicin alone reduced the growth rate of MCF-7 cells, but did not significantly affect angiogenesis. Doxorubicin in combination with A4.6.1 resulted in significant tumors regression. Histology indicated that some chambers lacked viable tumor cells at the end of the two week observation period, lending strong support that neutralization of VEGF in combination with conventional cytotoxic agents could be a new innovative treatment regimen for metastatic breast cancer.*

Targeting tumor microvasculature has become the focus of great interest as a therapeutic modality for the treatment of various malignancies since first proposed by Folkman over twenty years ago (1). Vascular endothelial growth factor (VEGF) is one potential target for the inhibition of tumor neovascularization as it is produced by the majority of human tumors (2). In a recent study (3), we showed that the blocking anti VEGF mAb, A4.6.1, completely inhibited formation of neovasculature and suppressed tumor growth of the human rhabdomyosarcoma cell line A673 in nude mice following an initial pre-vascular, angiogenesis independent growth phase. In a subsequent study, we demonstrated that A.6.4.1 also caused complete inhibition of angiogenesis and tumor growth of the prostate carcinoma cell line, DU 145 (4).

Recent data indicate that VEGF is secreted by human primary breast carcinomas (5) as well as by a variety of human breast carcinoma cell lines. (6, 7, 8). In women with breast cancer, there is a significant association between microvessel density and overall survivals as well as relapse free survival in both node-negative and node-positive patients. In node-negative patients, microvessel density correlates better with relapse-free survival than histological grade (8, 9, 10), making tumor microvessel density an excellent prognostic indicator. In addition, release of VEGF by breast tumors is closely associated with promotion of angiogenesis and with early relapse (9 ,11, 12).

Therapies targeting tumor neo-vasculature are often efective at blocking further tumor growth and metastatis. However, small, avascular tumors are often maintained in a "dormant" state (3, 13). To achieve complete eradication of such "dormant" foci, anti- angiogenic treatment may have to be combined with other treatment modalities such as

*This study complies with NIH guidelines for the care and use of laboratory animals.

*Correspondence to:* Per Borgström, Sidney Kimmel Cancer Center, 10835 Altman Row San Diego, CA 92121, USA. Phone: (619) 450-5990, ext. 245, Fax: (619) 450-3251.

*Key Words:* Vascular endothelial growth factor, anti-angiogenic, angiostatic, cytotoxic, combination, breast carcinoma, MCF-7, human, tumor spheroid, skinfold, intravital microscopy.

conventional cytotoxic drugs. The question however is whether, in the presence of effective anti-angiogenic agents with diminished blood perfusion of tumors, conventional cytotoxic drugs can be effective.

In the present study, we utilized intravital microscopy to evaluate the effectiveness of VEGF blockade alone or in combination with doxorubicin, a cytotoxic agent commonly used in the treatment of breast carcinoma, to eradicate tumors of human breast cancer cell lines implanted into nude mice.

## Materials and Methods

*Preparation of tumor spheroids.* The human breast carcinoma cell lines MCF-7, ZR-75, and SK-BR-3 were grown in DMEM (Dulbecco's Modification of Eagle's Medium, Gibco Labs., Grand Island, NY) containing 10% fetal calf serum (FCS, Gemini Bioproducts Inc., Calabasas, CA). Cultures were maintained in a humidified 5% CO2 atmosphere at 37 oC. Tumor spheroids were prepared as described previously (14). Briefly, suspensions of freshly trypsinized monolayers were pre-labeled with (5-(and-6)-((4-chloromethyl)benzoyl)amino)-tetramethylrhodamine (CMTMR, Molecular Probes Inc., Eugene, Oregon). Labeled cells were washed with fresh complete medium (DMEM + 10% FCS). A volume of 10 ml complete medium was added and the suspension (15 X 106cells/ml) placed into a 50 ml flask and rocked on a gyratory shaker in a humidified gas mixture of 5% CO2 and 95% room air at 37 oC. After 48 - 72 hours, round and solid tumor spheroids were formed. Selected spheroids of similar size were washed three times with PBS solution. This procedure insured that single spheroids of similar size were used for transplantation.

*Animal model and surgical techniques.* The dorsal skinfold chamber in the mouse was prepared as described previously (15, 16). In brief, male nu/nu mice (25-35 g body weight) were anesthetized (7.3 mg ketamine hydrochloride and 2.3 mg xylazine /100 g body weight, i.p.) and placed on a heating pad. Two symmetrical titanium frames were implanted onto a dorsal skinfold, so as to sandwich the extended double layer of skin. A 15 mm full thickness layer was excised. The underlying muscle (M. cutaneous max.) and subcutaneous tissues were covered with a glass cover slip incorporated in one of the frames. After a recovery period of 2-7 days, the coverslip of the chamber was removed and tumor spheroids were carefully placed over the upper tissue layer of the chamber and the chamber was closed again with the coverslip. The animals were housed individually in a room maintained at 21-22°C with free access to water and standard laboratory chow.

*Intravital microscopy.* Unanesthetized animals were immobilized in a plexiglass tube which was attached to the microscope stage (Leitz, Biomed). Fluorescence microscopy was performed using a Leitz Ploemopak epi-illuminator equipped with I2 and N2 filter blocks and video-triggered stroboscopic illumination from a xenon arc (Strobex 236, Chadwick Helmuth, Mountain View, CA). Observations were made using Nikon X4 (numerical aperture =0.10), Nikon X10 (NA=0.30) and Leitz X25 (NA=0.60) objectives. At the day of spheroid implantation, an overview video print (Sony Color Video Printer UP- 3000) was taken using a Leitz PL 1.6X (NA=0.05) objective and the position of the implanted spheroids were marked to facilitate future localization of tumors. Observations were performed 3, 7, and 14 days after implantation of the spheroids using 0.05-0.1 ml iv-injections of 2.5% FITC (fluorescein isothiocyanate)-Dextran 500,000 (Sigma, St. Louis, MO) to obtain vessel contrast enhancement. The dual labelling technique allowed precise identification of the rhodamine-labelled tumor cells and the study of tumor and microvessel growth. A silicon intensified target camera (SIT68, Dage-MTI, Michigan City, IN) was attached to the microscope and connected to a monitor (Panasonic TR-930). The experiments were recorded using a S-VHS video cassette recorder (JVC HR-S6600U) for off-line analysis of spheroid neo-vascularization.

Angiogenic activity induced by the implanted tumor spheroids was evaluated and scored according to below. 0.0 = No Response, 0.5 = Dilated capillaries, 1.0 = Dilated and tortuous capillaries, 1.5 = Early budding, 2.0 = Extensive budding, 2.5 = Extensive budding starting to form vascular network, 3.0 = Early vascular networks with flow, 3.5 = Established but heterogenous vascular network, 4.0 = Established vascular network, 4.5 = High density vascular network, 5.0 = Extremely high density vascular network.

*Image analysis.* For each spheroid, recordings were made using the Leitz X25 objective, which were used to calculate length, area and vascular density of the neovasculature being induced by the implanted tumor spheroids. To obtain the length of vessels within a microvascular network of a spheroid, a transparency was put in front of the monitor and a drawing was made using a pen (Sanford, Sharpie), taking great care to draw all vessel segments with the same line-width. Vessels from all focal planes within the microvascular network were drawn on the same transparency. Since the first signs of angiogenesis are dilation and tortuosity of the pre-existing underlying muscle capillaries, the transformed muscle capillaries were also included in these drawings. To obtain the area of the transformed and newly formed vessels, a second drawing was made of the same segment of the tumor. In this drawing the line width had the actual thickness of each vessel as displayed on the TV screen. All transparencies were scanned using a Hewlett- Packard Scanjet Plus scanner. The total number of black pixels was measured in each image file. Assuming equal line-width (drawing 1), this number is proportional to the length of the vascular network. In drawing 2, the total number of black pixels is proportional to the surface area. A calibration curve was constructed by making, with the same pen, drawings of known lengths and areas. Linear regression analysis were used to obtain the proportionality constants ($R^2$>0.999) for each parameter, under different magnifications. Vascular density was calculated by dividing the length of each vascular network by the area of tissue displayed on the TV screen. Total vascular length was calculated by multiplying vascular density by tumor area. Mean vessel diameter was obtained from the ratio between the area covered by newly-formed vessels and the total vascular length.

*Histology.* Tissue discs were fixed in 4% buffered formalin overnight. Representative full thickness blocks, taken at the tumor implant site, were processed for paraffin embedding. Five micron sections were cut for staining with hematoxylin and eosin.

*Statistical analysis.* The data was submitted to Normality and Equal Variance tests which revealed normal distribution. Statistical analysis was made using analysis of variance and multiple comparisons tests. For all tests, p values smaller than 5% were considered significant. Data are presented as mean ± SEM. Statistical calculations were computed with an statistical software package (SigmaStat, Jandel Scientific).

## Results

Figure 1 shows representative photomicrographs of MCF-7 cells implanted in the dorsal skinfold chamber. The left panels were obtained with the X4 objective (BG12 filter for enhancement of red blood cells). Right panels were obtained with the X25 objective (Plasma enhancement obtained with FITC-dextran). These photomicrographs

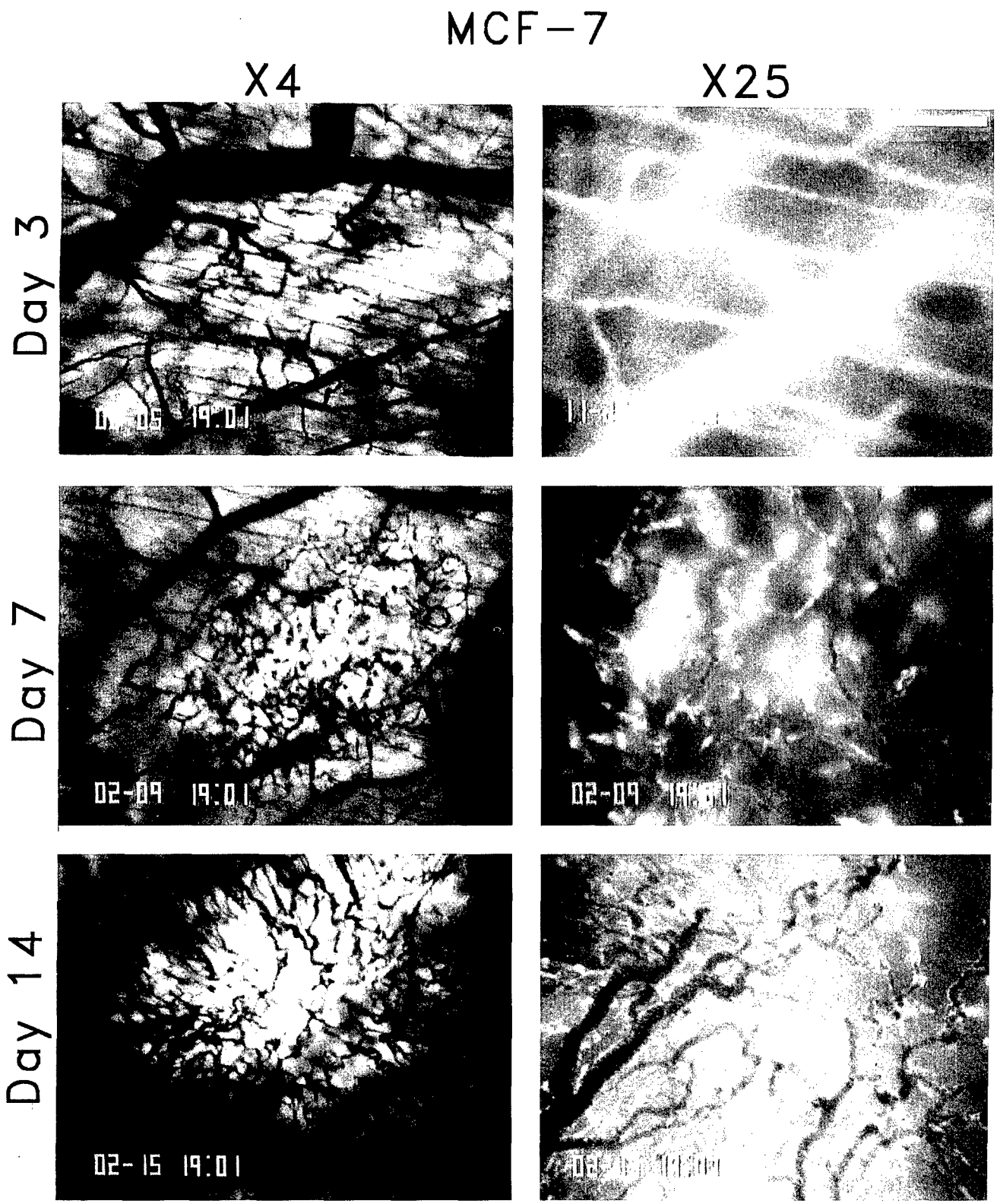


Figure 1. *Representative photomicrographs illustrating the characteristics of angiogenic activity induced by tumor spheroids of the MCF-7 cell line implanted in dorsal skinfold chambers in nude mice. White bar in left panels equals 500μm, and in right panels 100 m.*

illustrate the development of extensive tumor neovasculature after implantation of a microtumor. Within a day after implantation the first signs of angiogenesis appear, *i.e.,* dilatation and tortuosity of underlying muscle capillaries (upper panels) and shortly after, sprouts start to form from these transformed capillaries. The middle panels show the subsequent development of true neo-vasculature that matures into a vascular network with high vascular density. The lower panels illustrate formation of extensive vascular network at the tumor site.

Figure 2 illustrates the effects of blockade of VEGF with the anti-VEGF mAb

A.4.6.1 (A4.6.1 200 μg, given twice weekly i.p.) on angiogenic activity induced by MCF-7 cells. The left panels again illustrate the high angiogenic activity induced by MCF-7 tumor spheroids, with development of extensive neo-vasculature during the two-week observation period. The right panels illustrate the significant suppression of angiogenic activity accomplished after VEGF blockade, reducing extensive vascular networks with high capillary density in tumors of control animals to at most capillary budding in tumors of treated animals.

Similar results were obtained with the two other breast carcinoma cell lines, ZR-75, and SK-BR-3 (Figures 3 and 4).

Compiled data in terms of tumor area and angiogenic activity (arbitrary units, see Methods) for the three cell lines are summarized in Figure 5. Vertical dotted lines in left panels indicate transition from the initial pre-vascular angiogenesis independent growth phase (3 days) to the subsequent angiogenesis dependent vascular growth phase. The dashed lines in the right panels indicate the transition from early signs of angiogenesis in terms of morphological changes of pre-existing capillaries (dilation, budding) to formation of new capillary network.

This figure illustrates the following points; a) no inhibition of tumor growth occurs during the initial pre-vascular growth phase, b) no significant growth of tumors occurs in treated animals during the subsequent vascular growth phase, and c) in all three cell lines there is formation of extensive vascular networks in tumors of control animals, that is significantly suppressed to at most capillary budding after A4.6.1 treatment, *i.e.*, complete inhibition of angiogenesis (formation of true neovasculature).

Our previous data suggested that despite the complete inhibition of angiogenesis and tumor growth beyond the initial angiogenesis independent growth phase following treatment of animals with A4.6.1, dormant tumor seedlings always remained (6). We therefore also tested whether doxorubicin, a cytotoxic agent commonly used in the treatment of breast carcinoma, in combination with VEGF blockade, would be a more effective means to achieve complete tumor eradication than either treatment modality alone. Thus we investigated the effect of the blocking anti-VEGF mAb A4.6.1 (200 μg twice weekly i.p.), doxorubicin (5 mg/kg weekly i.v.), and the combination of the two, on growth and angiogenesis of tumor spheroids of MCF-7 cells implanted in dorsal skinfold chambers in nude mice.

Figure 6 shows representative histology of MCF-7 tumors from these experiments. Panel A - Control animals: Sections showed well formed nodules of poorly differentiated tumor abutting on the deep surface of sub-cutaneous skeletal muscle. Tumor cells had a vaguely packeted arrangement, were highly pleomorphic and frequent mitotic figures were seen. A prominent angiogenic response was associated with all tumors (arrowed). Panel B - A4.6.1 treated animals: Tumor nodules in all animals were smaller than in the controls, though the tumor cells had a similar cytological appearance to untreated animals. In two animals, occasional small capillary vessels were seen at the base of the tumor, in the other two animals there was no evidence of angiogenesis. Panel C - Doxorubicin treated animals: The appearance of the tumor cells was similar to controls and the tumor nodules were vascularized (arrowed). Panel D - Combination treatment, A4.6.1 and doxorubicin: The appearance of the tumor nodules in these animals was similar to those seen in groups B and C. Small vessels at the base of the tumor were observed in one of the four animals.

The growth of tumors in the various treatment groups over time is shown in the left panel of Figure 7. These data illustrate the following points: a) during the pre-vascular phase, tumors from all groups grew to the same extent, b) during the subsequent vascular phase, tumors in doxorubicin treated animals continued to grow although at a significantly suppressed rate ($p=0.011$), whereas in the A4.6.1 treated animals there was no significant growth of tumors ($p=0.087$). More importantly, the combination treatment actually resulted in shrinkage of tumor spheroids ($p<0.001$), and histology indicated that some of the chambers actually lacked viable tumor cells at the end of the two week observation period.

The right panel of Figure 7 depicts angiogenic activity. The data illustrate that in animals treated with anti-VEGF mAb there was significant suppression of angiogenic activity, from development of vascular networks with high capillary density to at most extensive budding.

Furthermore, the data illustrate that doxorubicin alone did not cause any significant suppression of angiogenesis, and, doxorubicin given with the anti-VEGF mAb further, interestingly, enhanced the anti-angiogenic effect of the anti-VEGF antibody, and the only signs of angiogenesis in this group, if any, were slight dilation of underlying muscle capillaries.

Figure 8 (left panel) shows vascular density at the tumor site at day 14. Vascular density ($cm^{-1}$) in the control, Doxorubicin, A4.6.1, and combination groups were 276.2±12.9, 225.0±18.2, 147.9±14.0 and, 69.7±23.6

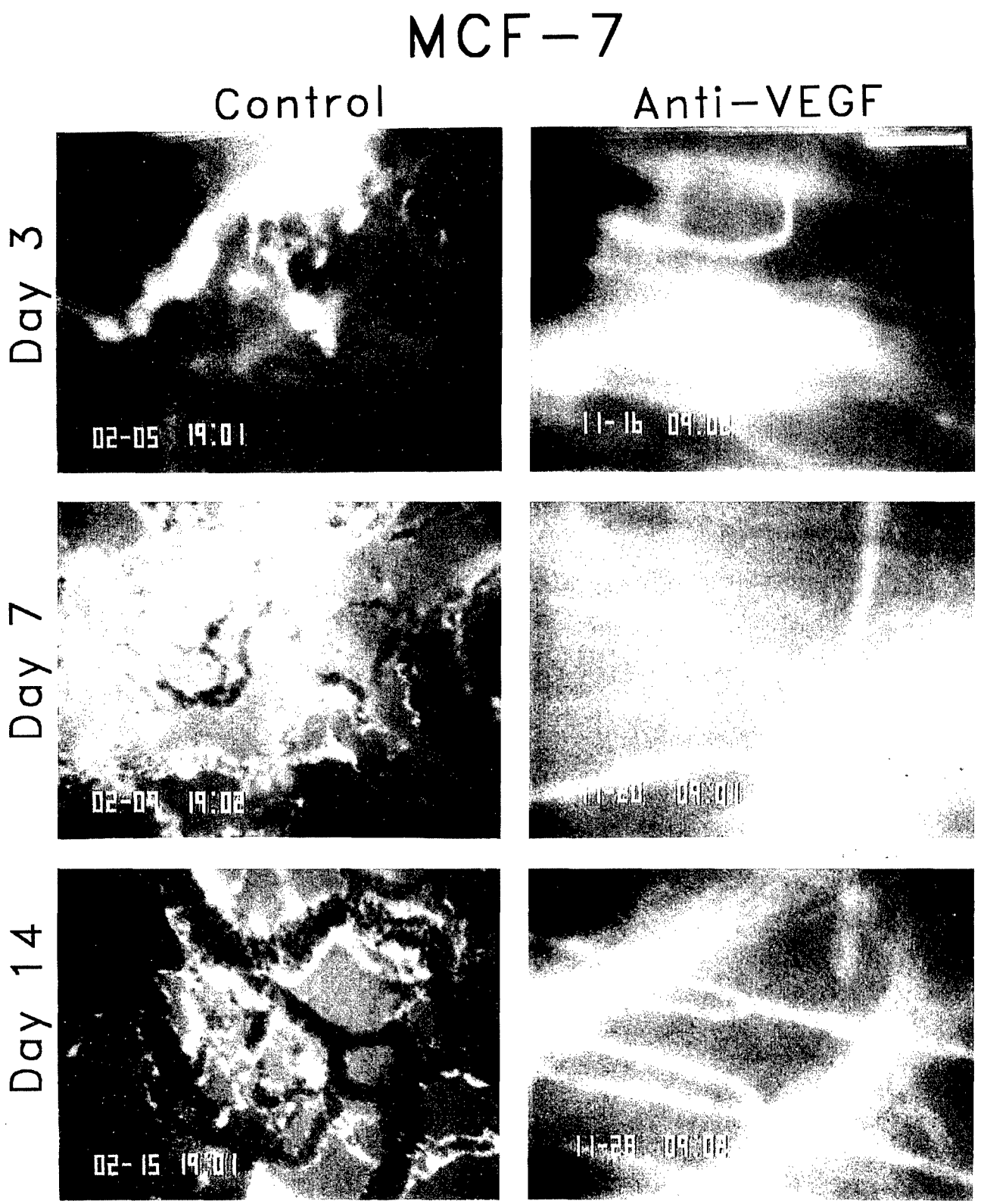


Figure 2. *Representative photomicrographs illustrating the effect of the blocking anti-VEGF mAb A4.6.1 on MCF-7 tumor spheroids implanted in dorsal skinfold chambers in nude mice. White bar equals 100μm.*

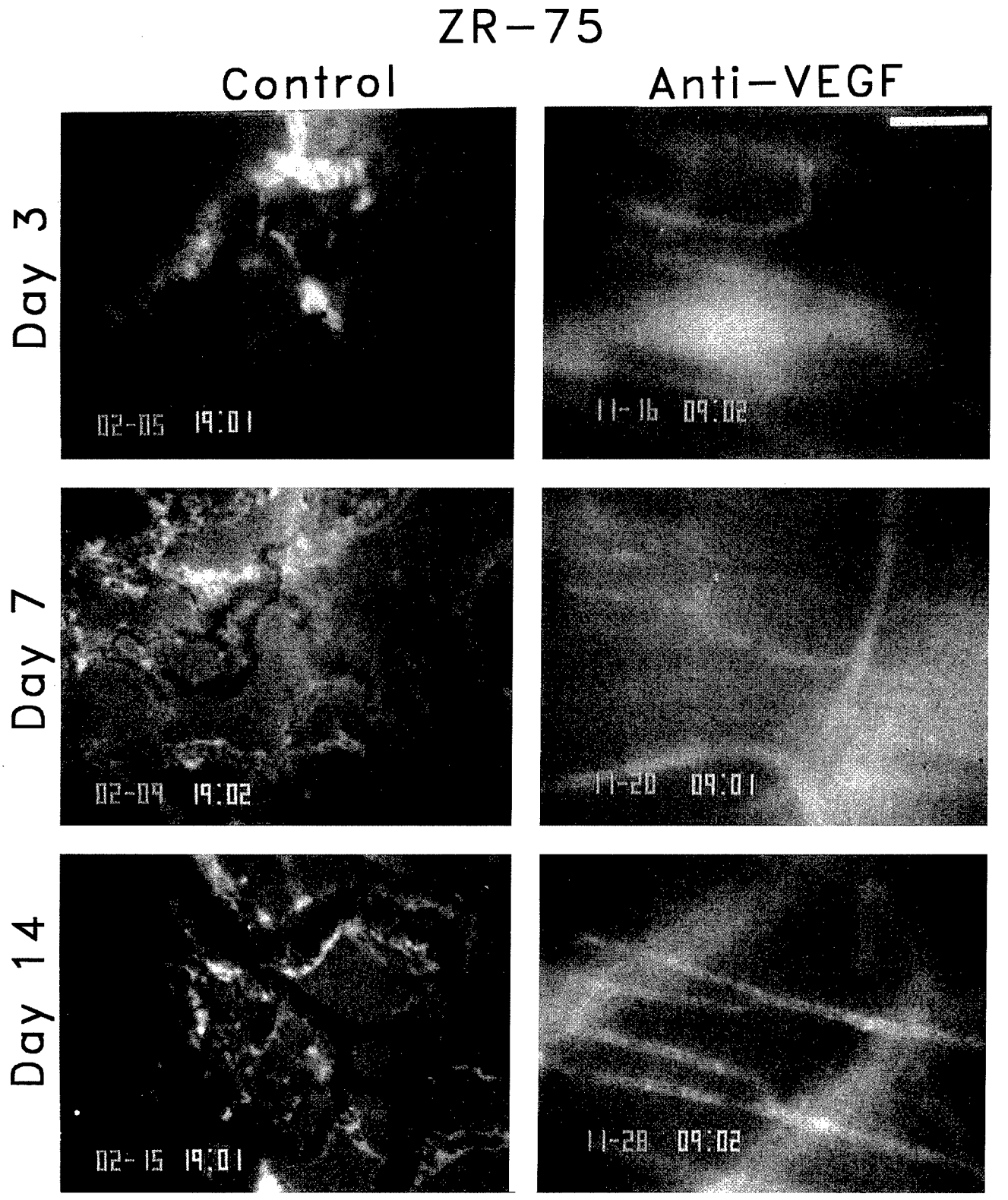


Figure 3. *Representative photomicrographs illustrating the effect of the blocking anti-VEGF mAb A4.6.1 on ZR-75 tumor spheroids implanted in dorsal skinfold chambers in nude mice. White bar equals 100μm.*

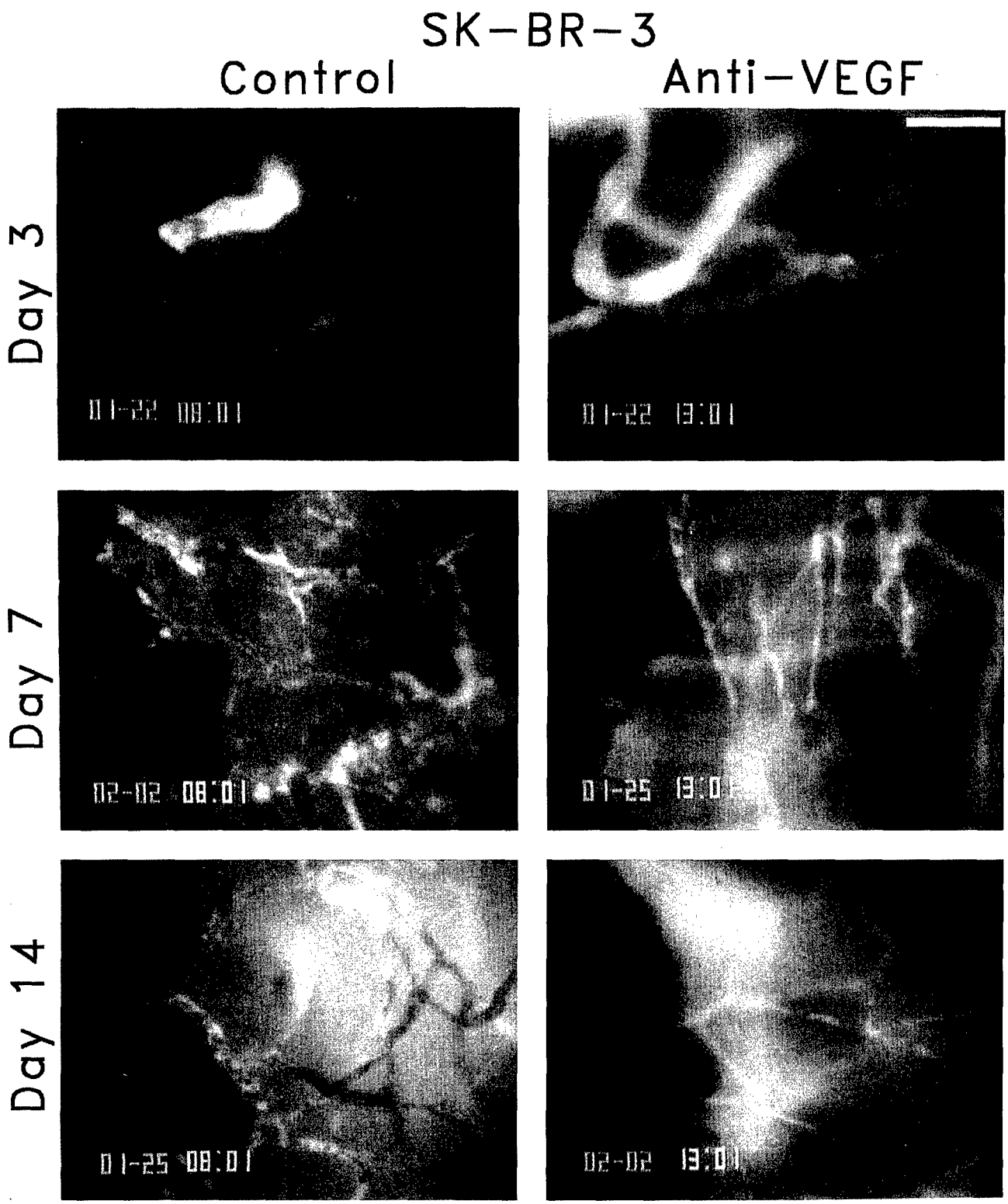


Figure 4. *Representative photomicrographs illustrating the effect of the blocking anti-VEGF mAb A4.6.1 on SK-BR-3 tumor spheroids implanted in dorsal skinfold chambers in nude mice. White bar equals 100μm.*

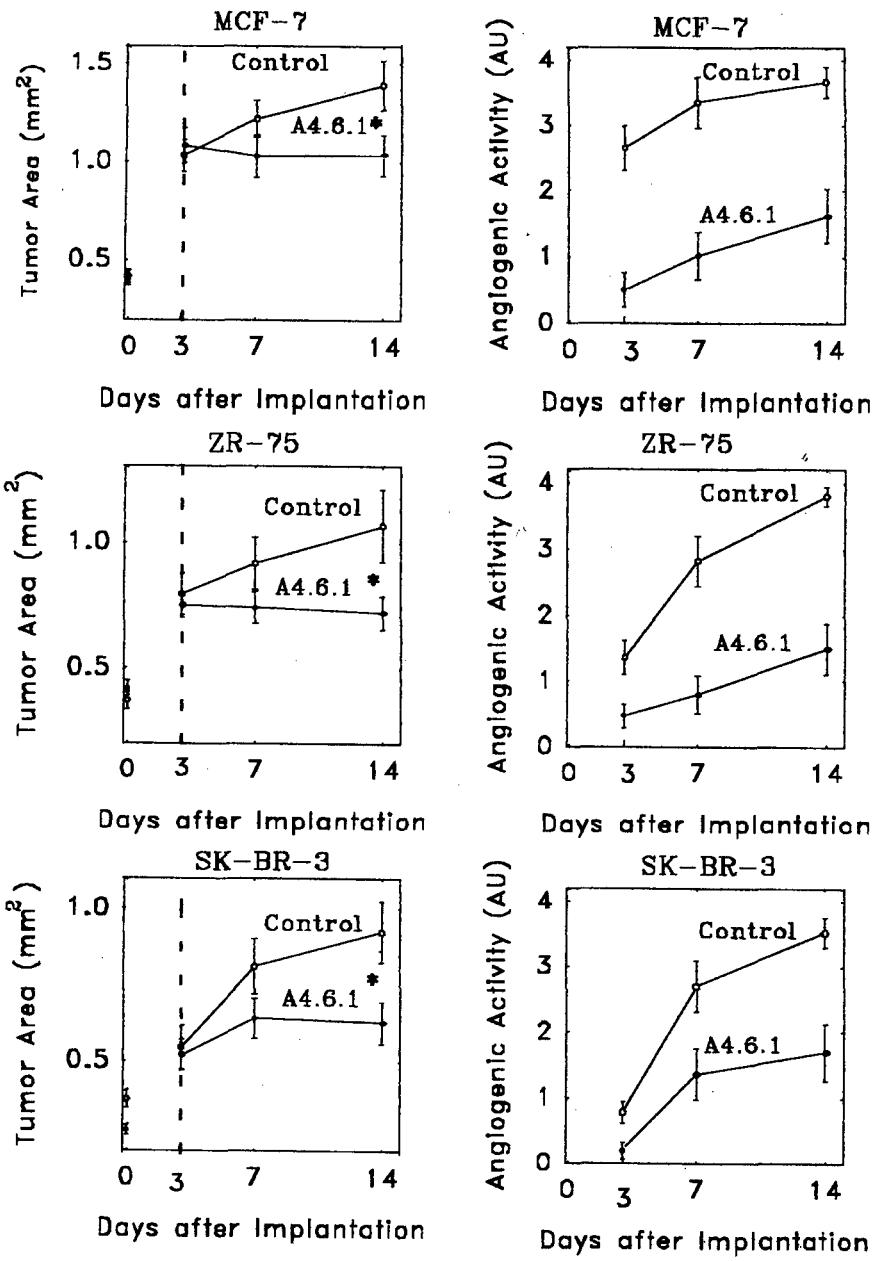


Figure 5. *Compiled data illustrating the effect of the blocking anti-VEGF mAb A4.6.1 on growth (tumor area; mm2) and angiogenic activity (arbitrary units, see Methods) of the human breast cancer cell lines MCF-7 (upper panels), ZR-75 (middle panels) and SK-B3-3 (lower panels), implanted in dorsal skinfold chambers in nude mice.*

respectively. The data illustrate that there was no significant reduction in vascular density in tumors of doxorubicin treated animals ($p=0.067$; *vs.* control), however, tumors in animals given the combination treatment had significantly lower vascular density compared to tumors of animals in the A4.6.1 group ($p<0.001$; *vs.* A4.6.1). Dashed line depicts vascular density of underlying muscle capillaries measured from 8 preparations ($208.4\pm17.3$ cm$^{-1}$).

The right panel of Figure 8 shows vascular area in percent of tumor area. Vascular area (%) in the control, A4.6.1, doxorubicin, and combination groups were $26.2\pm1.3$, $12.7\pm1.0$, $17.2\pm1.3$, and $4.4\pm2.8$ respectively. Vascular area of tumors in doxorubicin treated animals was significantly lower than that of tumors in control animals ($p<0.001$), due to a significantly narrower vessel diameter in tumors of doxorubicin treated animals $7.9\pm1.5$ *vs.* $9.2\pm1.7$; $p=0.05$). Vascular area of tumors in animals

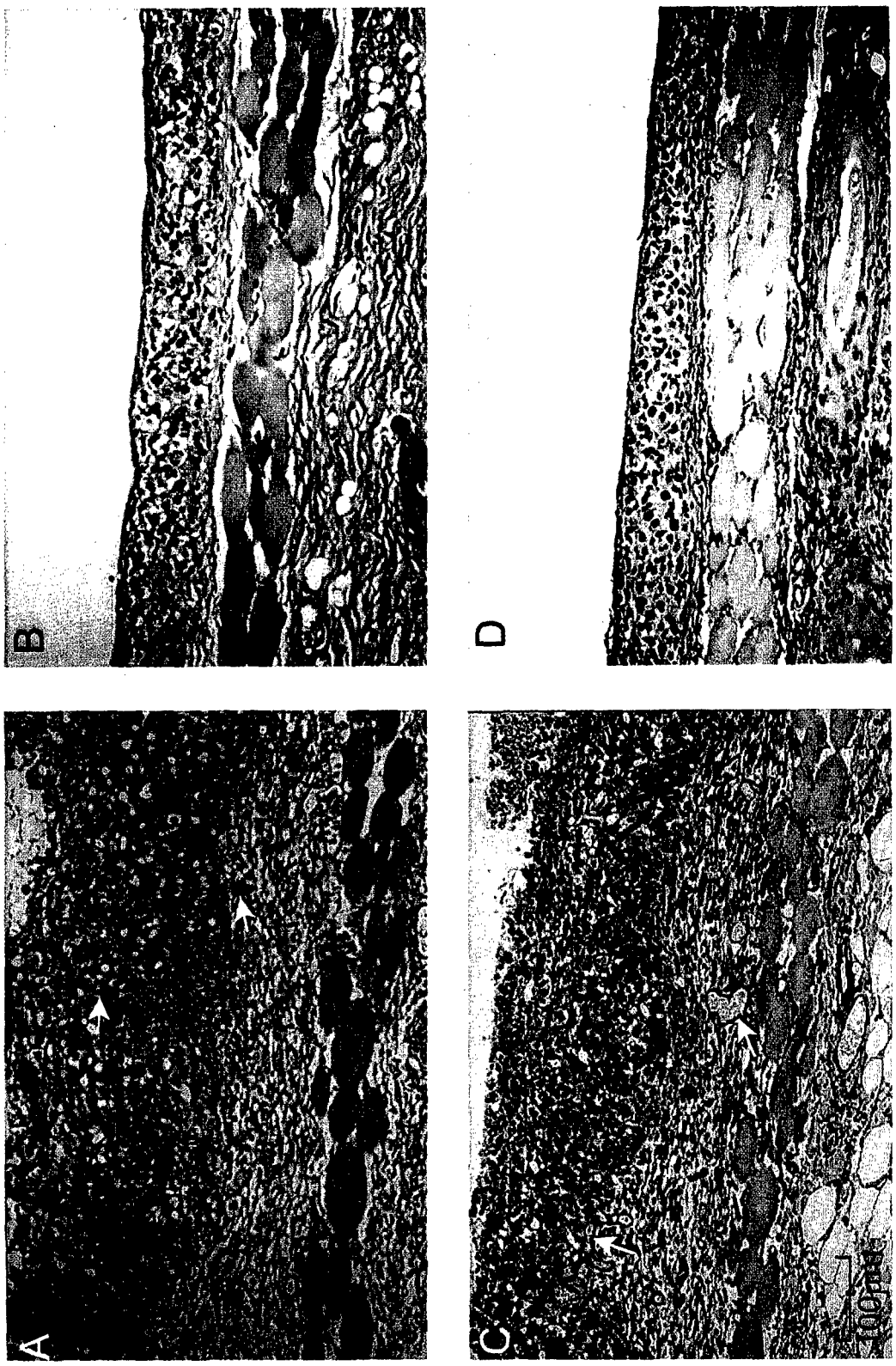


Figure 6. *Representative histology of MCF-7 tumor spheroids from, control animals (A), A4.6.1 treated animals (B), doxorubicin treated animals (C), and animals subjected to the combination treatment (D).*

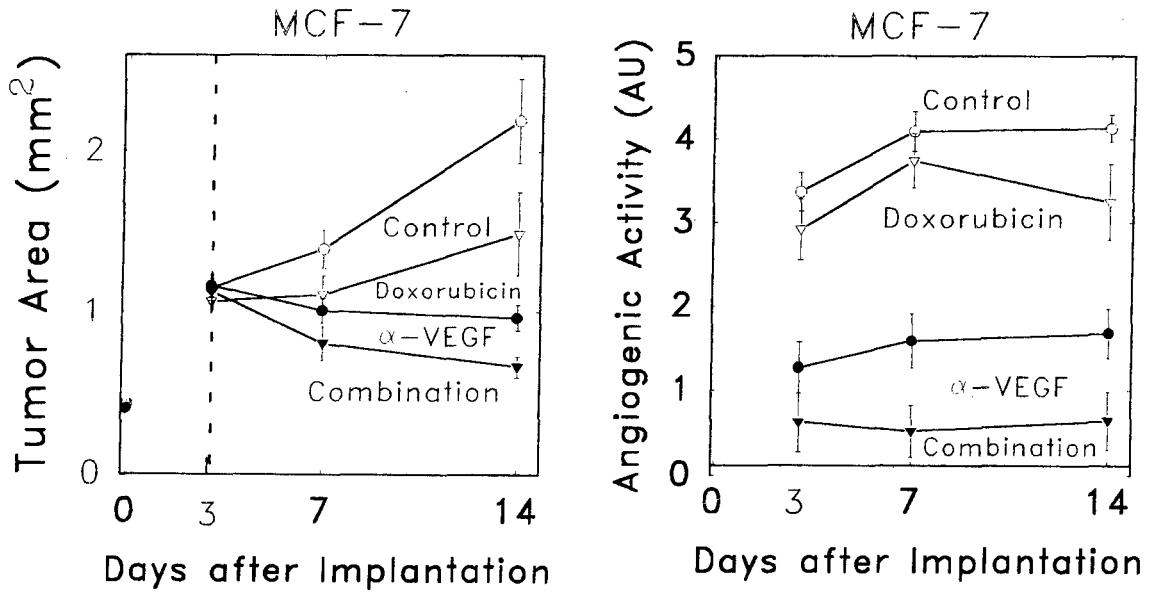


Figure 7. *Compiled data illustrating the effect of, the blocking anti-VEGF mAb A4.6.1, doxorubicin, and the combination of the two on growth and angiogenesis of MCF-7 tumor spheroids implanted in dorsal skinfold chambers in nude mice. The vertical dotted line in the left panel indicates the transition from the initial pre-vascular angiogenesis independent growth phase (3 days) to the subsequent angiogenesis dependent vascular growth phase (11 days). Dashed line in the right panel indicates transition from early signs of angiogenesis in terms of morphological changes of pre-existing capillaries (dilation, budding) to formation of new capillary network (neo-vasculature).*

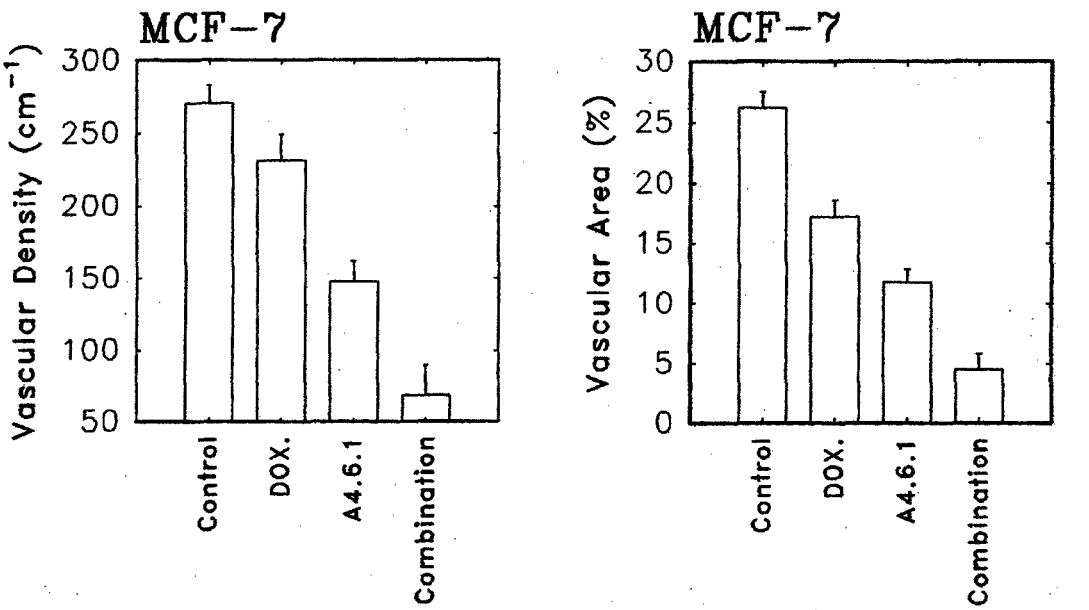


Figure 8. *The left panel shows vascular density at the tumor site ($cm/cm^2$) Dashed line depicts capillary density of underlying muscle capillaries. Angiogenic activity in A6.4.1 treated animals was completely inhibited to at most buddingThere was significant reduction of vascular density in tumors of A4.6.1 treated animals but no significant reduction in vascular density in tumors of doxorubicin treated animals. The right panel shows vascular area in percentage of tumor area, illustrating that tumors of animals subjected to the combination treatment had significantly lower vascular area than tumors of A4.6.1 treated animals.*

subjected to the combination treatment was significantly lower than that in anti-VEGF antibody treated animals ($p=0.001$). Vascular area of underlying skeletal muscle was $12.0\pm1.4$ %.

## Discussion

Over the last twenty years, numerous growth factors have been implicated to be important in tumor angiogenesis. However, recent data now suggests that VEGF plays a very critical role at least for certain cancer types. Previously we showed that for the human rhabdomyosarcoma cell line A673 (3), and the human prostatic cell line DU 145 (4), effective blockade of VEGF *alone*, caused complete suppression of tumor angiogenesis and inhibited further tumor growth beyond an initial pre-vascular angiogenesis independent growth phase. We also have unpublished data demonstrating that angiogenesis of certain colon carcinoma cell lines (SW480, MF-7), is completely VEGF dependent.

Results from the present study imply that VEGF also plays a critical role in breast cancer angiogenesis. Neutralization of VEGF *alone* is sufficient to achieve complete inhibition of human breast cancer angiogenesis in 3 different cell lines, causing complete cessation of tumor growth beyond the pre-vascular angiogenesis independent growth phase. However, our results also clearly demonstrate that microscopic dormant tumor colonies always remain even after effective anti-angiogenic treatment. These findings are similar to those of our previous study, where we presented histological data demonstrating that the morphological appearance of human rhabdomyosarcoma A673 cells implanted in mice treated with a neutralizing anti-VEGF mAb was similar to that observed in control animals, with marked nuclear atypia and frequent mitotic activity with mitotic indices in the order of 1-2% in tumors of both control and treated animals (3).

O'Reilly *et al* (13) have shown that systemic treatment with angiostatin; an angiogenesis inhibitor that selectively instructs endothelium to become refractory to angiogenic stimuli, caused an almost complete inhibition of tumor growth in mice. Similar to our studies, tumors in angiostatin treated mice regressed to microscopic dormant foci in which tumor cell proliferation was balanced by apoptosis.

Importantly, in the present study we are able to show that the dormant colonies remaining after VEGF blockade can be further reduced by combination of adriamycin. Adriamycin (doxorubicin), which is considered to be one of the most active and widely used agents in the treatment of breast cancer, causes a series of undesirable side effects that include cardiac toxicity, myelosupression and alopecia. In the present study 5 mg/kg given i.v., given weekly was a dose that gave significant growth inhibition, without causing severe side effects.

Our data illustrate that with the combination regimen utilizing complete blockade of VEGF, and a dose of doxorubicin that does not cause severe side effects, tumor spheroids actually shrink, and histology indicates that some of the chambers lack viable tumor cells at the end of the two week observation period.

The idea to combine anti-angiogenic therapy with conventional therapy is not novel. TNP-470, a synthetic analog of fumagillin has been shown to significantly potentiate the effect of cyclophosphamidecytotoxic (17). However, TNP-470 does not result in complete inhibition of angiogenesis. We are the first to investigate the consequences of a combination of *complete* inhibition of tumor angiogenesis and a cytotoxic agent to evaluate if such an agent could be effective in the absence of tumor neovasculature. and if so if thee would be an additative effect of the combination regimen.

In conclusion, results from the present study, support the concept that in breast cancer, neutralization of VEGF causes complete inhibition of angiogenesis. In addition, our data show that even with complete inhibition of angiogenesis, we at most achieve a state of prolonged dormancy of malignant cell colonies. However, combination therapies incorporating complete angiogenesis inhibition and conventional chemotherapy have the potential to provide therapeutically effective tumor killing, and thus could translate to new innovative treatment modalities to effectively cure metastatic breast cancer.

## Acknowledgements

The authors would like to thank Dale Winger for his excellent technical support.

## References

1 Folkman J: What is the evidence that tumors are angiogenesis dependent? J Natl Cancer Inst *82:* 4-6, 1990.

2 Ferrara N: The role of vascular endothelial growth factor in pathological angiogenesis. Breast Cancer Res Treat *36(2):* 127-37, 1995.

3 Borgström P, Hillan KJ, Sriramarao P, Ferrara F: Complete inhibition of angiogenesis and growth of microtumors by anti-vascular endothelial growth factor neutralizing antibody: Novel concepts of angiostatic therapy from intravital video microscopy. Cancer Res *56:* 4032-39, 1996.

4 Borgström P, Mario A, Bourdon Hillan KJ, Sriramarao P, Ferrara F:Neutralizing anti-vascular growth factor antibody completely inhibits angiogenesis and growth of human prostate carcinoma micro tumors *in vivo.* The Prostate, In Press, 1998.

5 Relf M, LeJeune S, Scott PAE, Fox S, Smith K, Leek R, Moghaddam A, Whitehouse R, Bicknell R, Harris AL: Expression of the angiogenic factors vascular endothelial cell growth factor, acidic and basic fibroblast growth factor, tumor growth factor 8-1, platelet-derived endothelial cell growth factor, placenta growth factor, and pleiotrophin in human primary breast cancer and its relation to angiogenesis. Cancer Res *57:* 963-969, 1997.

6 Conn G, Soderman D, Schaeffer MT, Wile M, Hatcher VB and

Thomas KA: Purification of a glycoprotein vascular endothelial cell mitogen from a rat glioma cell line. Proc Natl Acad Sci U.S.A. *87:* 1323, 1990.

7 Levy AP, Tamargo R, Brem H and Nathans D: An endothelial cell growth factor from the mouse neuroblastoma cell line NB41. Growth Factors *2(1):* 9, 1989.

8 Rosenthal RA, Megyesi JF, Henzel WJ, Ferrara N and Folkman J: Conditioned media from mouse sarcoma 180 cells contain vascular endothelial growth factor. Growth Factors *4:* 53-59, 1990.

9 Toi M, Kashitani J and Tominaga T: Tumor angiogenesis is an independent prognostic indicator in primary breast carcinoma. Int J Cancer *55(3):* 371-4, 1993.

10 Weidner N, Semple J and Folkman J: Tumor angiogenesis correlates with metastasis in invasive breast carcinoma. New Engl J Med *324:* 1-8, 1991.

11 Brown LF, Berse B, Jackman RW, Tognazzi K *et al:* Expression of vascular permeability factor (vascular endothelial growth factor) and its receptors in breast cancer. Hum Pathol 1995 *26(1):* 86-91, 1995.

12 Toi M, Hoshina S, Takayanagi T and Tominaga T: Association of vascular endothelial growth factor expression with tumor angiogenesis and with early relapse in primary breast cancer. Jpn J Cancer Res *85(10):* 1045-9, 1994.

13 O'Reilly MS, Holmgren L, Chen C, Folkman J: Angiostatin induces and sustains dormancy of human primary tumors in mice. Nat Med *2(6):* 689-92, 1996.

14 Torres Filho IP, Hartley-Asp B and Borgström P: Quantitative angiogenesis in a syngeneic tumor spheroid model. Microvasc Res *49:* 212-226, 1995.

15 Lehr H, Leunig M, Menger MD, Messmer K: Dorsal skinfold chamber technique for intravital microscopy on striated muscle in nude mice. Am J Pathol *143:* 1055-1062, 1993.

16 Leunig M, Yuan F, Menger MD, Boucher Y, Goetz AE, Messmer K and Jain RK: Angiogenesis, microvascular architecture, microhemodynamics, and interstitial fluid pressure during early growth of human adenocarcinoma LS174T in SCID mice. Cancer Res *52:* 6553-6560, 1992.

17 Teicher BA, Holden SA, Ara G, Sotomayor EA, Huang ZD, Chen YN, Brem H: Potentiation of cytotoxic cancer therapies by TNP-470 alone and with other anti-angiogenic agents. Int J Cancer *57(6):* 920-5, 1994.

*Received March 1, 1999*
*Accepted April 21, 1999*

ANTICANCER RESEARCH *18:* 4035-4042 (1998)

# Recombinant Platelet Factor 4, an Angiogenic Marker for Human Breast Carcinoma*

PER BORGSTRÖM[1], RICHARD DISCIPIO[2] and THEODORE E. MAIONE[3]

*[1]Sidney Kimmel Cancer Center, San Diego, CA 92121; [2]La Jolla Experimental Medicine, La Jolla, California 92037, and [3]Repligen, Cambridge, Massachusetts 02139, U.S.A.*

**Abstract.** *The present study was designed to test the hypothesis that rhPF4 binds with high specificity to the neovasculature of breast cancer carcinoma. To achieve this goal, we used intravital microscopy to study the binding characteristics of systemically injected fluorescently labeled rhPF4 (FITC-rhPF4) to the microvasculature of dorsal skinfold chambers in nude mice implanted with tumor spheroids prepared from the human breast cancer cell line MCF-7. Our results show that intravenously as well as intra-arterially injected FITC-rhPF4 exclusively labeled, with high intensity and specificity, the endothelium of the breast cancer induced neovasculature. Only on rare occasions (0.7 ± 1.5 site per cm$^2$ skinfold), short (37 ± 48 μm) intense labeled sites were found in the normal vasculature of the skinfold. Heparin could displace most of the label if injected within 10 min after the rhPF4-injection,but not 30 min after. In conclusion, our results show that rhPF4 preferentially binds to regions of active angiogenesis in vivo, supporting the concept of using rhPF4 conjugates to target tumors in cancer patients. Certain rhPF4 conjugates could have applications as imaging agents, with potential utility in identification, screening, detection, prognosis or staging of breast cancer and other cancers. Other similar conjugates, bearing therapeutic isotopes or toxins might be useful in selective treatment strategies.*

Breast cancer is the most commonly diagnosed cancer and the second leading cause of cancer death among women in the United States. With no current method of prevention available, early detection of breast cancer by screening mammography is of utmost importance, and the rate of breast cancer detection has accelerated due to the ability of mammography to identify nonpalpable breast lesions (1). A comparison of the results of clinical, roentgenological. cvtological and thermographic examination of breast cancer patients shows X-ray to be the most effective in making a reliable diagnosis. However, thermography, even though it gives a high percentage of false-negative and false-positive results, may contribute to the early detection of breast cancer and to the identification of women at high risk of developing breast cancer, since thermography detects the vascular responses (angiogenesis) associated with cancer growth (2).

Tumor growth and metastasis are angiogenesis-dependent. Virtually all solid tumors are neovascularized by the time they are detected. Tumors can not grow beyond a certain size without angiogenesis *i.e.*, once tumor take has occurred, every increase in tumor cell population must be preceded by an increase in new capillaries that converge upon the tumor (3, 4). Even a potentially malignant tumor can stay in a "dormant" stage for a number of years, with no invasion of surrounding tissue. The critical event that converts such a dormant tumor into a rapidly growing malignancy, is the switch to the angiogenic phenotype demarcating two stages in the development of the tumor - the prevascular phase and the vascular phase (5, 6). In breast cancer there is a significant association between microvessel density and overall survival and relapse free survival in both node-negative and node-positive patients. In node-negative patients microvessel density correlates better with relapse free survival than histological grade (7).

Many antigenic and genetic markers have been proposed for breast cancer, with potential utility in identihcation, screening, prognosis, detection, or monitoring. Those with the greatest promise include indicators of angiogenesis (8). rhPF4 is a recombinant protein with angiostatic activity, currently produced in *E. coli* in sufficient quantities to permit extensive preclinical and human testing. It has low acute and chronic toxicity and shows no clinically adverse reactions in human clinical trials.

In a previous study from this laboratory (9) we compared the binding of fluorescently (FITC) labeled rhPF4 to endothelial cells in culture and to the vasculature of the hamster cheek pouch *in vivo.* We found that binding of rhPF4 along the vasculature of the hamster cheek pouch was not uniform as would have been predicted from the *in vitro* findings. Instead, we found a low frequency of short,

*Correspondence to:* Per Borgström, Sidney Kimmel Cancer Center, 10835 Altman Row, San Diego, CA 92121, USA. Phone: (619) 450-5990 ext 245 Fax: (619) 450-3251.

*Key Words:* Platelet factor 4, breast carcinoma, human, angiogenesis-marker, anti-angiogenic, angiostatic, tumor spheroid, skinfold, intravital microscopy.

apparently specific, binding sites on arterioles and venules, which were intensely labeled with rhPF4; A tentative explanation proposed that these sites were regions of active angiogenesisJendothelial cell proliferation. A subsequent investigation directly evaluated the hypothesis that rhPF4 preferentially binds to regions of active angiogenesis/ endothelial cell proliferation (10). In that study we adopted an intravital microscopic model using the hamster skinfold preparation with implants of islets of Langerhans as inducers of angiogenesis. This model allowed detailed intravital microscopic analysis and quantitative evaluation of the revascularization process. Revascularization of implanted islets is complete within 14 days and the microvasculature is similar to that of islets *in situ*, appearing as glomerulus-like microvascular networks morphologically distinct from preexisting stable microvasculature. Using fluorescence microscopy, the binding and distribution of intravascularly injected FITC labeled rhPF4 on newly formed vessels was compared to that of the normal skin vasculature. The results demonstrated that systemically injected rhPF4 targets proliferating vascular regions with a high level of selectivity.

We have since developed an *in vivo* model for the quantitative study of the microvascular changes associated with the implantation of small tumor spheroids in skinfold chambers inserted in mice (11). The model allows detailed repeated *in vivo* observations of tumor neovasculature and permits quantitative evaluation of tumor growth and tumor angiogenesis *in vivo*.

The aim of the present study was to investigate the potential use of recombinant platelet factor 4 (rhPF4) as a marker for breast cancer angiogenesis and whether the use of a conjugated form of rhPF4 as a contrast medium could enhance or improve the early detection of breast cancer. Furthermore, since vessel density is an independent prognostic indicator in primary breast-cancer patients, the use of a rhPF4-conjugate as a contrast medium also could provide valuable information on which to base aggressive treatment decisions.

## Materials and Methods

*FITC labeling of rhPF4.* 5 mg rhPF4 (Repligen Corp., MA, USA) was diluted in 10 ml of 10 mM sodium phosphate buffer pH 7/150 mM NaCl. The protein was applied to a 5 ml column of heparin-Sepharose, and the column was washed with 2 volumes of sodium phosphate buffer. A solution of 10 mg/ml of 6-(fluorescein-5/6-carboxamido) hexanoic acid succinimidyl ester (Molecular Probes; Eugene, Oregon) was prepared in dimethylsulfoxide. Twenty five microliters of this solution was diluted into 1 ml of sodium phosphate buffer and applied immediately to the column containing the absorbed PF4. After 1 h at 23°C the column was washed with ~5 volumes of buffer (until the eluant was no longer yellow). Then the protein was eluted using 1.5 M NaCl in 10 mM sodium phosphate pH 7. The sample was dialyzed vs 25 mM sodium acetate pH 4/150 mM NaCl using dialysis tubing of a Mr=3000 cutoff (Spectrum Inc., Laguna Hills, CA). Amino acid analysis indicated 0.66 mg/ml which means that the correct concentration is 0.8-0.9 mg/ml.

*Preparation of tumor spheroids.* The human breast carcinoma cell line MCF-7 was grown in DMEM (Dulbecco's Modification of Eagle's Medium, Gibco Labs., Grand Island, NY) containing 10% fetal calf serum (FCS, Gemini Bioproducts Inc., Calabasas, CA). Cultures were maintained in a humidified 5% $CO_2$ atmosphere at 37°C. Tumor spheroids were prepared as described previously (11). Briefly, suspensions of freshly trypsinized MCF-7 monolayers were pre-labeled with (5-(and-6)-((4-chloromethyl)benzoyl)amino)-tetramethylrhodamine (CMTMR, Molecular Probes Inc., Eugene, Oregon). Labeled cells were washed with fresh complete medium (DMEM + 10% FCS). A volume of 10 ml complete medium was added and the suspension ($20 \times 10^6$ cells/ml) placed into a 50 ml flask and rocked on a gyratory shaker in a humidified gas mixture of 5% $CO_2$ and 95% room air at 37°C. After 24 - 48 hours, round and solid tumor spheroids were formed. Selected spheroids of similar size were washed three times with PBS solution and taken for either *in vivo* experiments or examination by light microscopy. This procedure insured that single spheroids of similar size were used for transplantation.

*Animal model and surgical techniques.* The dorsal skinfold chamber in the mouse was prepared as described previously (11). In brief, male nu/nu mice (25-35 g body weight) were anesthetized (7.3 mg ketamine hydrochloride and 2.3 mg xylazine /100 g body weight, i.p.) and placed on a heating pad. Two symmetrical titanium frames were implanted into a dorsal skinfold, so as to sandwich the extended double layer of skin. A 15 mm full thickness layer was excised. The underlying muscle (M. cutaneous max.) and subcutaneous tissues were covered with a glass cover slip incorporated in one of the frames. After a recovery period of 2-7 days, the coverslip of the chamber was removed and tumor spheroids were carefully placed over the upper tissue layer of the chamber and the chamber was closed again with the coverslip. The animals were housed individually in a room maintained at 21-22°C with free access to water and standard laboratory chow.

*Intravital microscopy.* The vasculature of the skinfold chamber was observed through a Leitz Biomed microscope (Leitz, Wetzlar, Germany) using 10X (Nikon, NA 0.3), 25X (Leik SW, NA 0.6) and 40X (Olympus, NA 0.7) salt water immersion objectives. Video recordings of the microcirculation were obtained from a silicon intensified target camera (SIT68, Dage-MTI, Michigan City, IN, USA), projected onto a monitor and stored on tape using a super-VHS video cassette recorder (JVC HC-S6600U, Japan). A time reference was stored on each frame (VTG-33, FOR-A Comp. LTD, Japan). The magnification from tissue to monitor was about 800-fold using the 40X objective, which was utilized for detection of fluorescent binding.

During bright field transillumination and using the previously taken photomicrographs the newly formed vessels of the tumors were identified. The newly formed vessels were easily detected since they geometrically contrasted with the skinfold vasculature. The latter having mainly straight paraliel capillaries while the newly formed vessels were more circular and regularly formed a network lying slightly above the focal plane of the normal skinfold vasculature.

For fluorescence purposes epi-illumination was used employing a Leitz Ploemopak epi-illuminator equipped with an 12 filter block and video-triggered stroboscopic illumination from a xenon arc (Strobex 236, Chadwick Helmuth, Mountain View, CA, USA). To be able to quantitatively follow the fluorescence intensity on newly formed vessels with time the above-mentioned SIT-camera was set in a manual sensitivity mode. This enabled a linear relationship between *in vivo* fluorescent intensity and gray scale brightness to be recorded on the videotape for analysis (see below).

*Experimental procedure.* On the day of the experiment, animals which were to be given FITC-labeled rhPF4 I.V., were administered with the desired dose in the tail vein, and placed in the Plexiglas tube, animals which were to be given FITC labeled rhPF4 i.a., were anesthetized with an i.p. injection of a mixture of Xylozine (10 mg/kg) and Ketamine (200 mg/kg) placed on a servo-controlled heating pad to maintain body temperature at 37 °C.

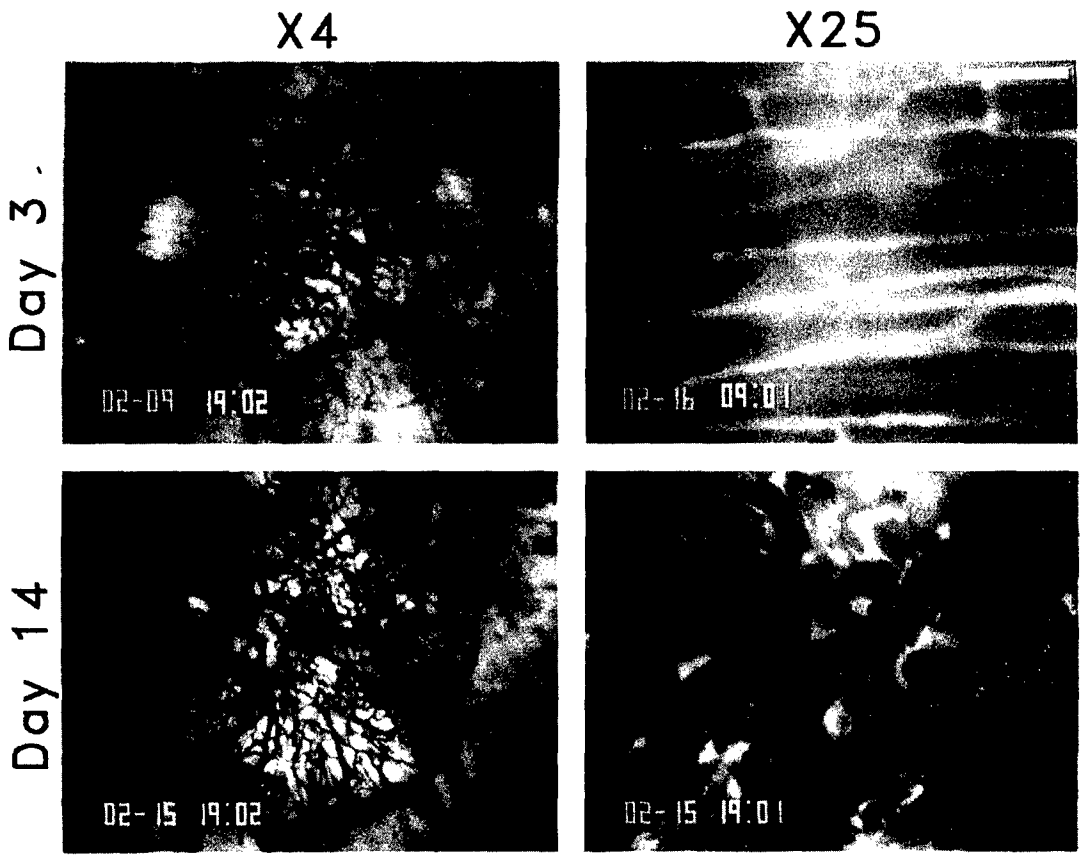


Figure 1. *Photomicrographs of MCF-7 tumor spheroids implanted in a dorsal skinfold chamber in a nude mouse 3 and 14 days after implantation. These photographs illustrate the extensive neo-vasculature formed at the tumor site. The upper right panel shows pre- existing muscle capillaries, and the lower panel the high density capillary density at the tumor site. White bar equals 500 μm, and 80 μm in left and right panels respectively*

The left carotid artery was cannulated for injection of FITC-labeled rhPF4. The animals were allowed to breathe room air freely. Supplemental anesthesia was given i.p. Vessels exhibiting normal flow, as opposed to sluggish or stagnant, were selected for study.

Experimental design. In the first series of experiments (Group 1; N=14), the animals were used 6-10 days after implantation of tumor spheroids when considerable neovasculature had already formed at the tumor sites. The FITC-labeled rhPF4 was injected into the tail vein in doses in the range from 1.5 to 15 mg/kg at a concentration of 0.9 mg/ml. The events in the vessels were recorded continuously during the first 5 min. Recordings thereafter were made at 15, 30, 60 and 120 min after rhPF4 injection. Each of 14 animals was given two different doses with an interval of two days in between.

In the second series of experiments 500 U heparin was given in the tail vein before (N=2), 4-9 min (N=3), or 30 min (N=3) after injection of rhPF4. The same registration protocol was used as described above for the animals of Group 1.

In the third series of experiments, animals were first given FITC labeled rhPF4 in the tail vein at a concentration of 6 mg/kg, two days later, they were given the same dose i.a. The same registration protocol was used as described above for the animals of Group 1.

In the fourth series of experiments, the binding characteristics of FITC-rhPF4 injected i.v. were evaluated in chambers without tumor implants (N=6) as a control. These chambers were scanned over in an effort to find intensely lebeled sites.

*Analysis of vascular interaction.* In order to investigate the intensity and time course of the labeling of rhPF4 to newly formed vessels and to the normal skinfold vasculature, the vasculature was analyzed off-line from the video recording using photodensitometric computer software (Optimas 4.1, Bioscan Inc, Edmonds, WA). The software also allowed the measurement of vessel length.

A line generated on the video screen was positioned across a chosen vessel. The line was gray scale sensitive along its entire length and generated a densitometric value pixel by pixel. Due to the labeling of vessel walls, two densitometric peaks were obtained for each cross-section, which contrasted with the dark lumen of the vessel. The two peaks were identified as well as a mean of the lumen value. By averaging the two peaks and subtracting this value with the lumen value, one absolute fluorescence value was obtained per cross-section. A similar analysis was performed with unlabeled vessels of the normal skinfold vasculature to obtain a background value, which was subtracted from the values obtained from labeled vessels. For each tumor and for each time period investigated, 4 subjectively chosen cross-sections were analyzed in an identical manner. For each time period chosen the mean fluorescence value was computed, resulting in one mean fluorescence value per animal. Since maximal labeling intensity occurred 3-5 minutes after rhPF4 injection, and our previous investigation (10) showed that plasma rhPF4 levels out after 5 minutes, the labeling intensity of vessels at 5 min was set to 100 %. The fluorescence intensity readings at 15, 30, 60 and 120 min post-injection was then expressed as a percentage of the reading at 5 min. Half-life of labeling intensity was calculated from the slopes (ß)

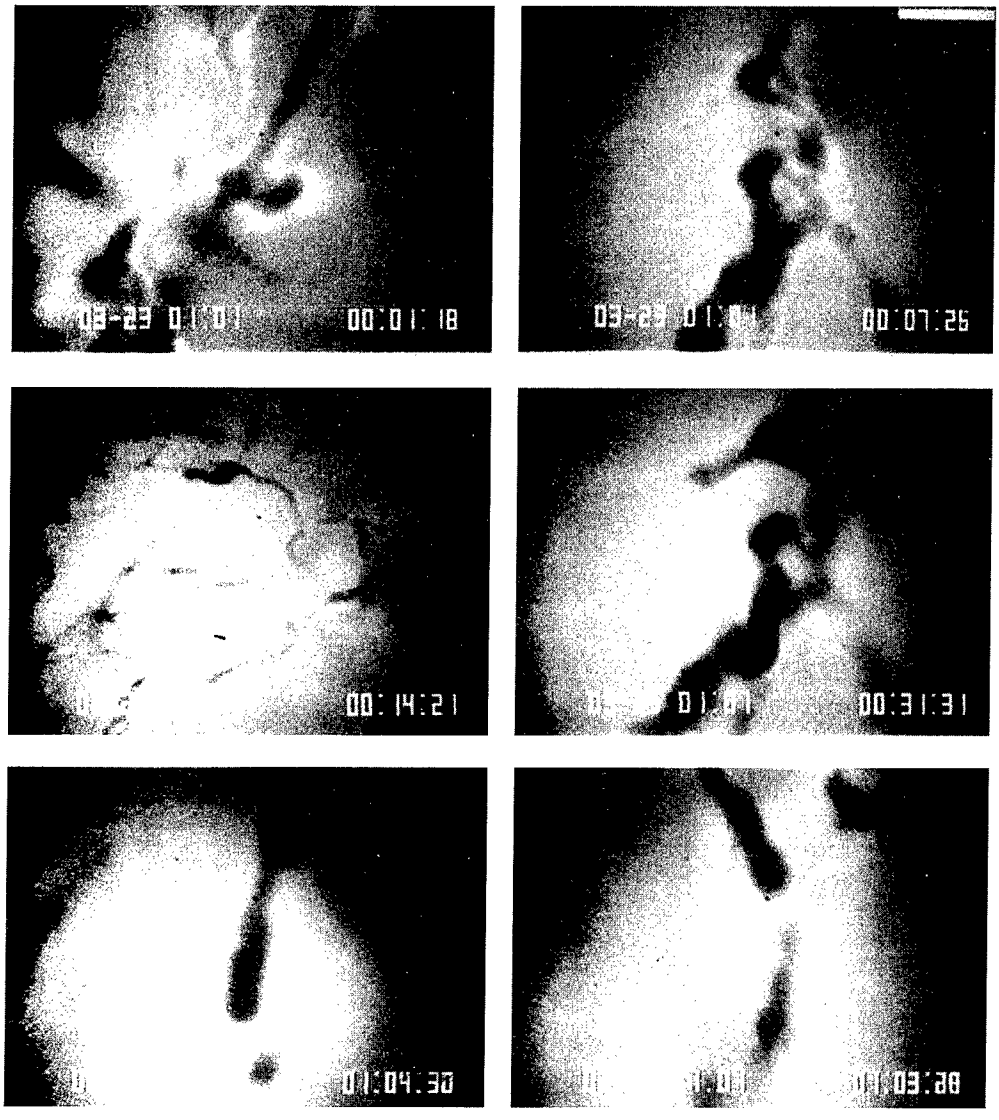

Figure 2. *Photomicrographs obtained after injection of 6 mg/kg FITC-rhPF4, illustrating the selective binding of FITC-rhPF4 to newly formed tumor capillaries. White bar equals 200 μm in lower left panel, and 80 μm in the other panels.*

of individual intensity curves obtained by linear regression of labeling intensity) as a function of time. Half-life ($T_{1/2}$) was calculated as: $T_{1/2}= \ln(2)/ß$.

*Documentation of vascular interaction.* Representative photomicrographs from the labeling of rhPF4 on vascular structures were obtained off-line from the video recordings using a video printer (Sony UP-3000, Japan). In some cases the image was enhanced for clarity of presentation using an integrator (Dage-MTI, DSP 200, Michigan City, IN, USA).

*Statistical analysis.* The data was submitted to Normality and Equal Variance tests, which revealed normal distribution. Statistical analysis was made using analysis of variance and multiple comparisons tests. For all tests, $p$ values smaller than 5% were considered significant. Data are presented as mean ± SEM. Statistical calculations were computed with an statistical software package (SigmaStat, Jandel Scientific).

## Results

Figure 1 shows photomicrographs of MCF-7 tumor spheroids implanted in a dorsal skinfold chamber in a nude mouse 3 and 14 days after implantation, demonstrating the temporal development of the tumor spheroid and associated neovasculature. The photomicrographs were obtained with a blue filter (BG12) for red blood cell enhancement (left panels), or alternatively FITC-dextran 500 was used for plasma enhancement (right panels). The development of extensive neovasculature during the two week observation period was observed on a regular basis (left panels). The pre-existing muscle capillaries clearly contrasted with the high density capillary network at the tumor site (lower right panel).

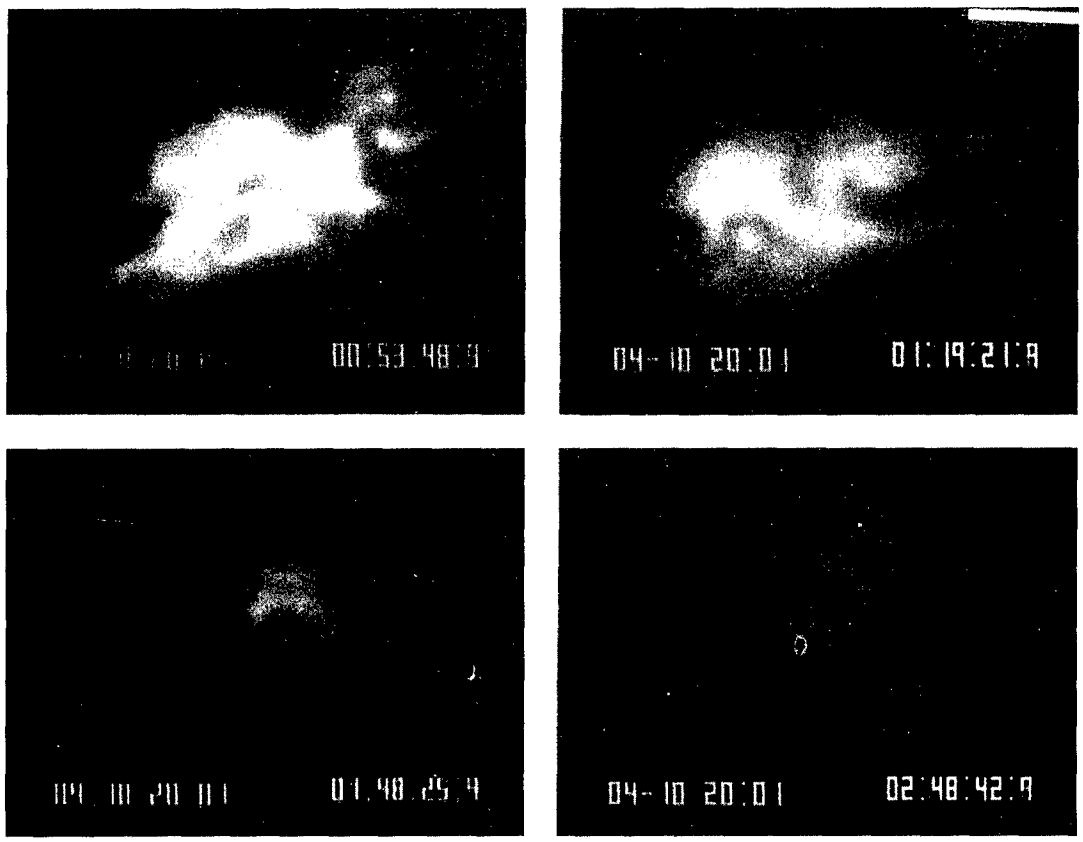


Figure 3. *Representative photomicrographs obtained 5, 30, 60 and 120 min after injection of 15 mg/kg FITC-rhPF4, illustrating the time-course of the selective FITC-rhPF4 labeling of tumor capillaries. White bar equals 50 μm.*

In the first series of experiments, FITC-rhPF4 was injected i.v. at various dose levels in the range from 1.5 to 15 mg/kg. Injections were given between 6 and 10 days after implantation of the tumor spheroids. Figure 2 shows representative photomicrographs from one such experiment (6 mg/kg), illustrating the selective binding to newly formed tumor capillaries. Figure 3 demonstrates the time course of labeling after an I.V. injection of 15 mg/kg FITC-rhPF4. The photomicrographs were obtained 5 min, 30 min, 1h and 2 hours after the injection, illustrating the rapid intense labeling associated with the neovascular network of the tumor obtained after i.v. injection and the decline during the 2 h observation period. Consistent with our previous studies (9, 10), binding of FITC-rhPF4 to other vascular sites was generally transient and of substantially lower intensity (data not shown).

At each dose level, fluorescence associated with MCF-7 induced neovasculature was visible and quantifiable at the 5 and 10 min time points (Figure 4). By the initial time point for all doses the plasma phase fluorescence had declined substantially from the initial pulse of plasma fluorescence seen within 30 sec of the bolus injection, permitting the clear visualization of fluorescence to the surface of the vascular lumen. Binding to non- neovascular capillary endothelial surfaces in the observation field was generally of significantly lower initial intensity and essentially fully depleted by the initial (5 min) measurement time point. The presence of fluorescence specifically associated with the neovasculature, however was persistent and measurable for up to 2 h in the neovasculature of animals treated at 6 to 15 mg rhPF4/kg (Figure 4).

The maximal luminescence associated with the neovascular sites increased almost linearly with dose over the concentration range tested at the earliest ffme points measured (Figure 5). These data imply that either binding sites were not saturated at the highest dose levels, or that the concentration of rhPF4 by internalization or translocation processes occurred in parallel to the initial binding event.

The half life of decay of fluorescent signal intensity also increased approximately proportionally to dose level (Figure 6) further suggesting the presence of a dose dependent sequestration process. The initial binding of fluorescently labeled protein (6 mg/kg dose) was substantially reversed by administration of heparin (5000 U/kg) within 5 minutes after FITC-rhPF4 injection. Administration of heparin at 30 min after FITC-rhPF4 injection failed to

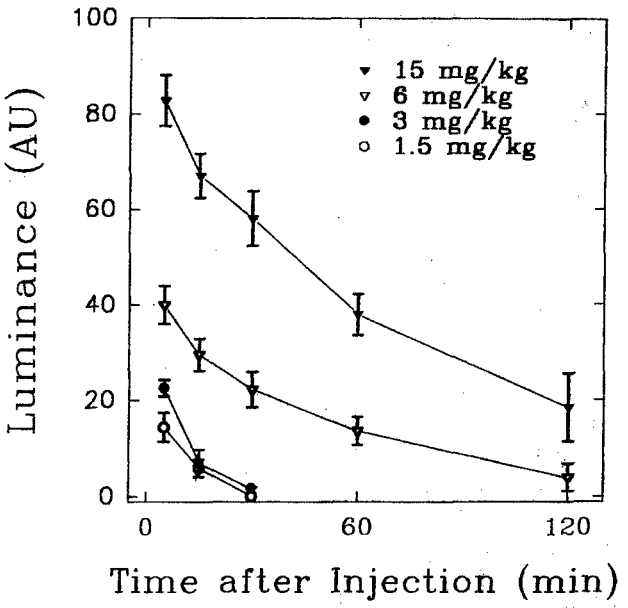


Figure 4. *Compiled data of time curves obtained after I.V. injection of FITC-rhPF4 in the range from 1.5 to 15 mg/kg. 15 mg/kg labeled with high intensity and specificity, the endothelium of the neovasculature induced by the MCF-7 cells. The lowest dose (1.5 mg/kg) was clearly visible 5 min after injection but subsided during the first 30 min.*

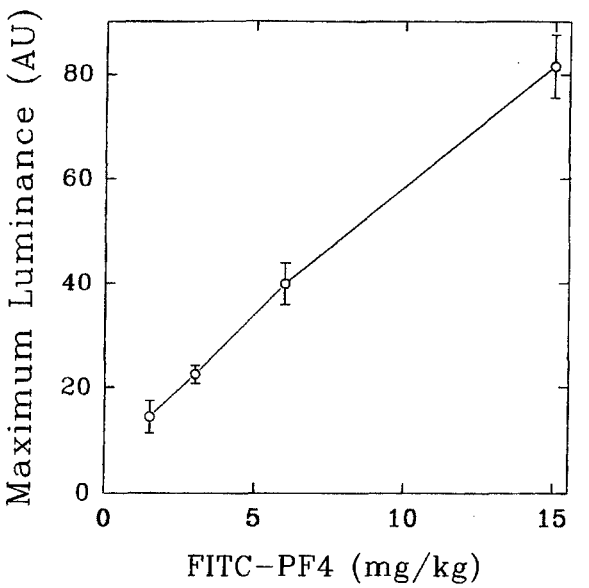


Figure 5. *Maximum luminance showed an almost linear relabonship in the dose range from 1.5 to 15 mg/kg, indicating no saturation in labeling intensity.*

reverse the accumulation of fluorescent signal in the neovascular structures.

No significant differences were seen in the pattern, timing or intensity of neovascular labeling by FITC-rhPF4 (6 mg/kg) between intravenous and intra-arterial administration routes (data not shown).

## Discussion

The present study was designed to test the hypothesis that rhPF4 binds with high specificity to neovasculature of breast cancer carcinoma grown in nude mice similar to results seen with non-tumor induced neovasculature in other animal models (9, 10). Our results clearly demonstrate that FITC-rhPF4 selectively labels the neovasculature of small tumor spheroids of the human breast cancer cell line MCF-7, implanted in dorsal skinfold chambers in nude mice consistent with the conclusion that rhPF4 preferentially binds to actively dividing endothelial cells. These results provide strong support for the use of rhPF4-binding as a marker for breast cancer angiogenesis and suggest that the use of a conjugated rhPF4 as a contrast medium could facilitate the early detection of breast cancer with high neovascularity and pathogenic potential. In the present investigation, the combined use of video-microscopy and fluorescently labeled rhPF4 allowed us to characterize in detail the binding patterns of intravascular rhPF4 in growing tumor tissue as a model for its possible future development as a clinical

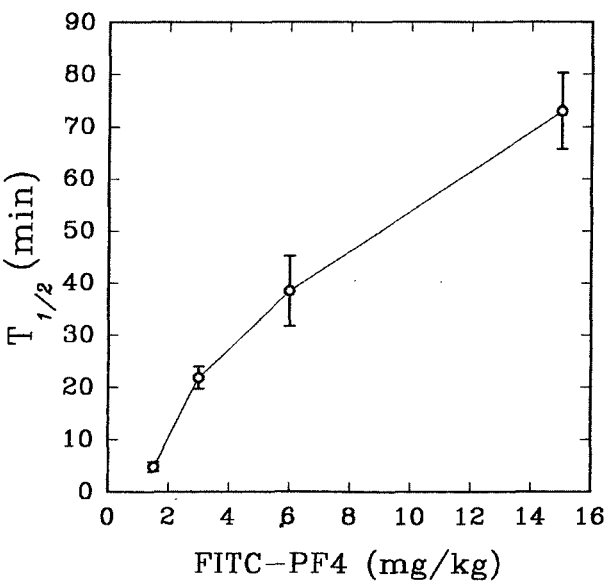


Figure 6. *Half-life (T1/2) as a function of dose of FITC-rhPF4, demonstrating an almost linear increase in half-life of labeling intensity.*

imaging agent. An agent with distinct selectively for binding to new or active vascular growth could potentially find utility in initial diagnosis, prognosis, staging and treatment of aggressively growing tumors if combined to powerful therapeutic modalities.

A comprehensive knowledge of PF4 structural features has permitted the identification of several preferred conjugation sites that permit the covalent modification of the protein while preserving its native angiostatic activity. rhPF4 conjugates created for imaging purposes retain their ability to block endothelial cell proliferation *in vitro* and would presumably also produce therapeutic angio-inhibiting effects at its binding sites that could be potenffated by coupling powerful therapeutic isotopes or toxins as a treatment strategy coupled to the novel imaging approach. Other similar conjugates of rhPF4 also retain biological activities based on *in vitro* human umbilical vein endothelial cell (HUVEC) proliferation assay (unpublished data), supporting the concept that conjugates with appropriate properties can be developed for *in vivo* roentgenological or MRI examination techniques as well as novel therapeutic applications or *in vitro* histological staging.

The circulation half-life of rhPF4 is biphasic and consists of a 2 minute fast phase and a 30 minute terminal phase (9). The rapid plasma clearance rate exhibited by core protein is thus well suited for development as a targeting molecule permitting rapid diagnostic application with minimal background plasma noise.

The pharmacology of rhPF4 also is well documented. Its general lack of toxicity has been clinically documented in at least 80 humans in the presence or absence of heparin. No dose-limiting clinical adverse reactions occurred during the first 24 h or within 7 days. Acute toxicity assessments at 100 mg/kg and chronic assessment at 3.5 mg/kg daily for 28 days in rabbits showed no adverse side effects specifically associated with rhPF4 treatment (unpublished data). rhPF4 has been tested in humans as a heparin reversal agent in multiple clinical settings (12) and as a therapeutic angiogenesis inhibitor in multiple cancer patient populations (13). Overall, the core protein has been well tolerated in these studies, supporting its further expansion as a basic plafform for the development of novel imaging agents or its use as neovascular tumor drug delivery vehicle.

In a recent study Ruoslahti *et al* coupled doxorubicin to peptides that home specifically to tumor blood vessels and showed that the effficacy of doxorubicin was enhanced against human breast cancer xenografts in nude mice (14). The selectivity of rhPF4 binding to neovascular endothelium might also offer an opportunity to reduce the toxicity and improve the therapeutic index of a wide variety of chemotherapies whose utility is limited by their nonspecific distribution and toxicity. Recent demonstrations of tumor vascular indices as important prognostic markers for breast (7) and other cancer types including melanoma (15), prostate carcinoma (16) and non-small-cell lung cancer (17), supports the aggressive exploration of agents such as rhPF4 that selectively binds to newly established capillary beds. If sufficient sensitivity and specificity can be established in patients, neovascular targeting agents may offer an important new strategy for detection of occult primary tumors and metastases as well as for staging of tumors detected by other means.

## Acknowledgements

The authors would like to thank Dale Winger for his excellent technical support. This study was supported by grant I.-0493 from the Breast Cancer research Program, University of California, and in part by NIH grant AI 22415

## References

1 Sailors DM, Crabtree JD, Land RL, Rose WB, Burns RP, Barker DE: Needle localization for nonpalpable breast lesions. Am-Surg *60(3):* 186-9, 1994.
2 Gautherie M, Haehnel P, Walter JP, Keith LG: Thermovascular changes associated with *in situ* and minimal breast cancers. Results of an ongoing prospective study after four years. J-Reprod-Med. 833-42, 1987
3 Folkman J: Angiogenesis. *In:* Biology of Endothelial Cells, E.A. Jaffe, Ed. (Nijhoff, Boston), 412-428, 1984.
4 Folkman J: What is the evidence that tumors are angiogenesis dependent? J Natl Cancer Inst *82:* 4-6, 1990.
5 Chodak GW, Haudenschild C, Gittes RF and Folkman J: Angiogenic activity as a marker of neoplastic and of preneoplastic lesions of the human bladder. Ann Surg *192:* 762-71, 1980.
6 Folkman J: *In:* Xlth Congress of Thrombosis and Haemostasis (Verstraete, M, Vermylen, J, Liijnan, R and Amout, J, eds.) Leuven, Belgium: Leuven University Press 583-96, 1987.
7 Weidner N, Semple J and Folkman J: Tumor angiogenesis correlates with metastasis in invasive breast carcinoma. New Engl J Med *324:* 1-8, 1991.
8 Hayes DF: Tumor markers for breast cancer. Ann-Oncol *4(10):* 807-19, 1993.
9 Hansell P, Olofsson M, Maione M, Arfors K-E, and Borgstrom P: Differences in binding of platelet factor 4 to vascular endothelium *in vivo* and proliferating endothelial cells *in vitro.* Acta Physiol Scand *154:* 449-459, 1995.
10 Hansell P, Maione TE and Borgstrom P: Selective binding of platelet factor 4 to regions of active angiogenesis *in vivo.* Am J Physiol *269:* H829-36, 1995
11 Torres Filho IP, Hartley-Asp B and Borgstrom P: Quantitative angiogenesis in a syngeneic tumor spheroid model. Microvasc Res *49:* 212-226, 1995.
12 Dehmer GJ, Fisher M, Tate, DA, Teo S, Bonnem E: Reversal of Heparin Anticoagulation by Recombinant Platelet Factor 4 in Humans. Circulation vol: 91, pp: 2188-2194, 1995.
13 Northfelt DW, Robles R, Lang W, Wagner B, Kahn J and Bonnem E: Multicenter Phase II Study of Intravenous (A/) Recombinant Platelet Factor 4 (rPF4 in AIDS-Related Kaposi's Sarcoma(AIDS-KS) Proceedings of the American Society of Clinical Oncologists (ASCO), vol 14, p. 288 (abstract), 1995.
14 Arap W, Pasqualini R, Ruoslathi E: Cancer Treatment by targeted drug delivery to tumor vasculature in a mouse model. Science *279:* 377-389, 1998.
15 Srivastava A, Laidler P, Davies RP, Horgan K and Hughes LE: The prognostic significance of tumor vascularity in intermediate-thickness (0.76-4.0 mm thick) skin melanoma. A quantitative histologic study. Am J Pathol *133(2):* 419-23, 1988.
16 Weidner N, Caroll PR, Flax J, Blumenfeld W and Folkman J: Tumor angiogenesis correlates with metastasis in invasive prostate carcinoma. Am J Pathol *143:* 401-409, 1993.
17 Macchiarini P, Fontanini G, Hardin MJ, Squartini F and Angeletti CA: Relation of neovascularisation to metastasis of non-small-cell lung cancer. Lancet *340(8812):* 145-6, 1992.

*Received June 2, 1998*
*Accepted July 6, 1998*

1-10
The Prostate 35:000–000 (1998)

# Neutralizing Anti-Vascular Endothelial Growth Factor Antibody Completely Inhibits Angiogenesis and Growth of Human Prostate Carcinoma Micro Tumors In Vivo

Per Borgström,[1]* Mario A. Bourdon,[1] Kenneth J. Hillan,[2] P. Sriramarao,[1] and Napoleone Ferrara[2]

[1]*La Jolla Institute for Experimental Medicine, La Jolla, California*
[2]*Genentech Inc., South San Francisco, California*

**BACKGROUND.** Neovascularization mediated by growth factors produced by tumors is critical for the growth of tumors. Vascular endothelial growth factor (VEGF) is one such growth factor. A neutralizing anti-VEGF antibody (A4.6.1) was recently shown in vivo to inhibit tumor angiogenesis and growth of the human rhabdomyosarcoma cell line A673. The antibody profoundly changed the growth characteristics of the tumor line from a rapidly growing malignancy to a dormant microcolony.
**METHODS.** In the present study, we evaluated the effects of A4.6.1 (100 μg twice weekly, i.p.) on growth and angiogenic activity of spheroids of the human prostatic cell line DU 145 (diameter 700 μm at implantation) implanted in dorsal skinfold chambers in nude mice (n = 11). An antibody of the same isotype (n = 5) or saline (n = 5) was used as control. Tumor cells were prelabeled with a fluorescent vital dye (CMTMR), which allowed measurement of size of the implanted tumor spheroids throughout a two week observation period. FITC-dextran was used for plasma enhancement to visualize angiogenic activity.
**RESULTS.** Tumors of control animals induced a neo-vasculature with high vascular density (350 ± 12 $cm^{-1}$). In animals treated with the anti-VEGF antibody, there was complete inhibition of neovascularization of the micro tumors and complete inhibition of tumor growth after the initial prevascular angiogenesis independent growth phase.
**CONCLUSIONS.** These results demonstrate that inhibition of the key regulatory paracrine growth factor for endothelial cells, VEGF, results in complete suppression of prostate cancer induced angiogenesis and prevents tumor growth beyond the initial prevascular growth phase. *Prostate* 35:000–000, *1998.* © 1998 Wiley-Liss, Inc.

1-10

*KEY WORDS:* **vascular endothelial growth factor; anti-angiogenic; angiostatic, prostate; human; tumor spheroid; skinfold; intravital microscopy**

## INTRODUCTION

Cancer of the prostate is a major malignancy in men in the Western world. After lung cancer, it is the second most common cause of death due to cancer in the United States. By the time prostate cancer is diagnosed, about 30–60% of patients have local extracapsular extension or distant metastases [1]. The effectiveness of available treatments today is uncertain. Stage C and stage D disease are often incurable, and the efficacy of treatment for stage B prostate cancer is doubtful. Currently available evidence about the effectiveness of radical prostatectomy, radiation therapy, and hormonal treatment derives largely from case series reports without proper controls [2–5]. Digi-

Contract grant sponsor: National Institutes of Health; Contract grant number: CA52879

*Correspondence to: Per Borgström, La Jolla Institute for Experimental Medicine, 11077 North Torrey Pines Road, La Jolla, CA 92037

Received 13 March 1997; Accepted 11 June 1997



PROD #97-028

tal rectal examination (DRE) was the principal screening test for prostate cancer until elevations in certain serum tumor markers such as prostate-specific antigen (PSA) became a new means of screening for prostate cancer [6]. However, with current screening techniques, there is no evidence that screening and early detection results in reduced morbidity or mortality, in part because few studies have prospectively examined the health outcomes of screening. There is therefore a great need for improved screening techniques as well as novel means to treat prostate cancer.

Recent data suggest a significant association between microvessel density and overall survival and relapse-free survival [7]. Furthermore, data show that an angiogenesis inhibitor such as Linomide suppresses not only growth of primary tumors, but also metastatic spread as well as the growth rate of established metastases [8–10]. These data strongly suggest angiogenesis as a novel prognostic indicator and angiogenesis inhibitors as new effective approaches to treat prostate cancer.

Vascular endothelial growth factor (VEGF) is a potent angiogenic factor that has been identified as a key regulatory paracrine growth factor for endothelial cells [11,12]. In a recent study, we showed that treatment with a blocking monoclonal antibody, specific for VEGF, completely inhibited neovascularization of microtumors from the human rhabdomyosarcoma cell line A 673 implanted in dorsal skinfold chambers in Beige mice [13]. Furthermore, the anti-VEGF antibody suppressed the growth of these tumors to the extent that tumors implanted in treated animals could not grow beyond a critical volume of <1 $mm^3$; that is, the anti-VEGF antibody dramatically changed the growth characteristics of the tumor line from being a rapidly growing malignancy to being a dormant micro colony.

Recent data have demonstrated that prostate cell lines secrete VEGF in vitro [14,15], but to date little is known about the role of VEGF in in vivo prostate cancer angiogenesis. The purpose of the present study was to determine whether angiogenesis induced by human prostatic cancer cells can be suppressed by blockade of VEGF. To achieve this goal, microspheroids of the human prostatic cell line DU 145 were implanted in dorsal skinfold chambers in nude mice that were either treated with the anti-VEGF antibody A4.6.1, a control antibody of the same isotype (6E10) or saline given by the intraperitoneal route twice weekly.

## METHODS

### Preparation of Tumor Spheroids

The human prostate cell line DU 145 was grown in Dulbecco's Modification of Eagle's Medium (DMEM)

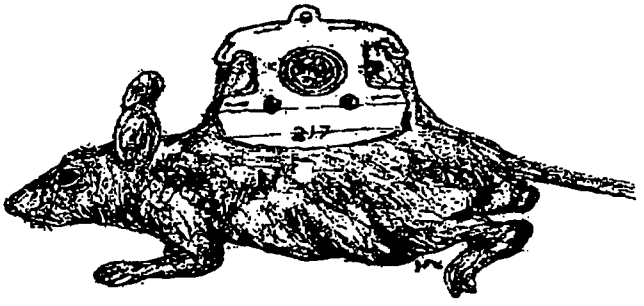

**Fig. 1.** Cartoon illustrating the dorsal skinfold chamber in nude mice. This model permits detailed repeated in vivo observations of angiogenesis and permits quantitative evaluation of tumor growth and tumor angiogenesis in vivo.

(GIBCO, Grand Island, NY) containing 10% fetal calf serum (FCS) (Gemini Bioproducts, Calabasas, CA). Cultures were maintained in a humidified 5% $CO_2$ atmosphere at 37°C. Tumor spheroids were then prepared as described previously [13]. Briefly, individual cells were prelabeled with (5-(and-6)-(((4-chloromethyl)benzoyl)amino)tetra methylrhodamine (CMTMR) (Molecular Probes, Eugene, OR) in a suspension of trypsinized DU 145 monolayer cells. Labeled cells were then washed with fresh complete medium (DMEM + 10% FCS). A volume of 10 ml complete medium was added and the suspension ($2 \times 10^7$ cells/ml) placed into a 25-ml flask and rocked on a gyratory shaker in a humidified gas mixture of 5% $CO_2$ and 95% room air at 37°C. After 48–72 hr, round and solid tumor spheroids were formed. Selected spheroids with similar diameters were then washed three times with phosphate-buffered saline (PBS) solution. A handpicking procedure insured single spheroids of similar size for transplantation.

### Animal Model and Surgical Techniques

The dorsal skinfold chamber in the mouse (Fig. 1) was prepared as described in detail previously [16,17]. In brief, male Beige nude/xid mice (25–35 g body weight) were anesthetized (7.3 mg ketamine hydrochloride and 2.3 mg xylazine/100 g body weight, i.p.) and placed over a heating pad. Two symmetrical titanium frames were implanted onto a dorsal skinfold so as to sandwich the extended double layer of skin. One layer was completely removed in a circular area of 15 mm in diameter. The underlying thin layer of muscle (M. cutaneous max.) and the subcutaneous tissue were covered with a coverslip incorporated in one of the frames. After a recovery period of 2–7 days, the coverslip of the chamber was removed and spheroids

were carefully placed over the upper tissue layer of the chamber and the chamber was closed again with the coverslip. The animals were housed individually in a room maintained at 21–22°C with free access to water and standard laboratory chow.

### Treatment Regimen

A neutralizing monoclonal anti-VEGF antibody A.4.6.1 [11] was injected by the intraperitoneal route at a dose of 100 mg twice weekly, starting the day of tumor implantation. As controls, an antibody of the same isotype (6E10) or PBS were used.

### Intravital Microscopy

Unanesthetized animals were immobilized in a plexiglass tube attached to the microscope stage (Leitz, Biomed). Fluorescence microscopy was performed using a Leitz Ploemopak epi-illuminator equipped with I2 and N2 filter blocks and video-triggered stroboscopic illumination from a xenon arc (Strobex 236, Chadwick Helmuth, Mountain View, CA). Observations were made using Nikon ×4 (numerical aperture = 0.10), Nikon ×10 (NA = 0.30) and Leitz ×25 (NA = 0.60) objectives. At the day of spheroid implantation, an overview video print (Sony Color Video Printer UP-3000) was taken using a Leitz PL 1.6X (NA = 0.05) objective, and the position of the implanted spheroids was marked to facilitate future localization of tumors. Observations were performed at 3, 7, and 14 days after implantation of the spheroids, using 0.05- to 0.1-ml intravenous injections of 2.5% fluorescein isothiocyanate (FITC)-Dextran 500,000 (Sigma Chemical Co., St. Louis, MO) to obtain vessel contrast enhancement. The dual labeling technique allowed precise identification of the rhodamine-labeled tumor cells and the study of tumor and microvessel growth. A silicon-intensified target camera (SIT68, Dage-MTI, Michigan City, IN) was attached to the microscope and connected to a monitor (Panasonic TR-930). The experiments were recorded using a S-VHS video cassette recorder (JVC HR-S6600U) for off-line analysis of spheroid neo-vascularization.

Angiogenic activity induced by the implanted tumor spheroids was evaluated and scored as follows: 0.0, no response; 0.5, dilated capillaries; 1.0, dilated and tortuous capillaries; 1.5, early budding; 2.0, extensive budding; 2.5, extensive budding starting to form vascular network; 3.0, early vascular networks with flow; 3.5, established but heterogenous vascular network; 4.0, established vascular network; 4.5, high-density vascular network; and 5.0, extremely high-density vascular network.

### Image Analysis

For each spheroid, recordings were made using the Leitz ×25 objective, which were used to calculate the length, area, and vascular density of the neovasculature induced by the implanted tumor spheroids. To obtain the length of vessels within a microvascular network of a spheroid, a transparency was put in front of the monitor, and a drawing was made using a pen (Sanford, Sharpie), taking great care to draw all vessel segments with the same linewidth. Vessels from all focal planes within the microvascular network were drawn on the same transparency. Since the first signs of angiogenesis are dilation and tortuosity of the pre-existing underlying muscle capillaries, the transformed muscle capillaries were also included in these drawings. To obtain the area of the transformed and newly formed vessels, a second drawing was made of the same segment of the tumor. In this drawing the line width had the actual thickness of each vessel as displayed on the TV screen. All transparencies were scanned using a Hewlett-Packard Scanjet Plus scanner. The total number of black pixels was measured in each image file. Assuming equal linewidth (drawing 1), this number is proportional to the length of the vascular network. In drawing 2, the total number of black pixels is proportional to the surface area. A calibration curve was constructed by making, with the same pen, drawings of known lengths and areas. Linear regression analysis were used to obtain the proportionality constants ($R^2$ >0.999) for each parameter, under different magnifications. Vascular density was calculated by dividing the length of each vascular network by the area of tissue displayed on the TV screen. Total vascular length was calculated by multiplying vascular density by tumor area. Mean vessel diameter was obtained from the ratio between the area covered by newly-formed vessels and the total vascular length. Tumor volume (V) was calculated according to $V = 2/3 \times A \times h$, where A is the tumor area and h the thickness of the tumor. In preliminary experiments, spheroid thickness after implantation was estimated as 40.5 ± 11.7% of the tumor diameter.

### Histology

Tissue discs were fixed in 4% buffered formalin overnight. Representative full-thickness blocks, taken at the tumor implant site, were either processed for paraffin embedding or immersed overnight in 15% sucrose and then frozen and embedded in OCT medium; 5-μm sections were cut at 100-μm intervals from each and stained with hematoxylin and eosin (H&E).

Mike

### Statistical Analysis

The data were submitted to Normality and Equal Variance tests which revealed normal distribution. Statistical analysis was made using analysis of variance and multiple comparisons tests. For all tests, $P$ values smaller than 5% were considered significant. Data are presented as mean ±SEM. Statistical calculations were computed with an statistical software package (SigmaStat, Jandel Scientific).

## RESULTS

Tumor spheroids of the human prostate cell line DU 145 with an initial diameter of about 700 mm were implanted in dorsal skinfold chambers in nude mice (Fig. 1). In one group of animals (n = 11) the, neutralizing monoclonal anti-VEGF antibody A.4.6.1 was injected by the intraperitoneal route at a dose of 100 mg twice weekly, starting the day of tumor implantation. As controls, an antibody of the same isotype (6E10) (n = 5) or PBS (n = 5) was used.

Figure 2 shows representative photomicrographs of tumor spheroids from these experiments. Figure 2 (top left) presents an overview, obtained at the day of implantation using the Leitz 1.6× objective (epi-illumination, N2 filterblock), illustrating the in vivo labeling of tumor cells with CMTMR. To facilitate localization of the tumor spheroid, over the existing microvascular network, simultaneous transillumination with filtered blue light (BG12) is superimposed. Figure 2 (top right) shows the tumor spheroids at 3 days after implantation, using the Nikon 4× objective (epi-illumination, N2 filterblock). Figure 2 (middle left), obtained with the Nikon 10× objective (epi-illumination, N2 filterblock) illustrates the intense CMTMR labeling of tumor cells at 7 days after implantation. Figure 2 (middle right) shows the same tumor spheroid using epi-illumination (N2 filterblock) with FITC-dextran to obtain plasma enhancement. In the upper section of this photomicrograph, the tortuous tumor neovasculature can be seen, contrasting the pre-existing underlying muscle capillaries seen in the lower section. Figure 2 (bottom left) was obtained outside the tumor area, showing pre-existing straight muscle capillaries. Figure 2 (bottom right) shows the tumor area illustrating the higher vascular density at the tumor site.

Figure 3 presents photomicrographs of tumor spheroids from the control group (left) and from the group treated with the anti-VEGF antibody (right), taken at 3 days (top), at 7 days (middle), and at 14 days (bottom) after implantation, using the Leitz 25× objective. In these photomicrographs, vascular enhancement was obtained with FITC-dextran (epi-illumination, I2 filterblock), which allows visualization of the microvasculature. Figure 3 (top left) shows that, in the control group, at 3 days after implantation, there are dilated and tortuous capillaries with extensive budding, whereas in the treated group, there is only slight dilation of the capillaries. At 7 days after implantation, there is an established vascular network in the control group, compared with slightly dilated capillaries with some tortuosity in the treated animals (Figure 3, middle). At 2 weeks after implantation, tumor spheroids implanted in control animals have induced a neovasculature with extremely high vascular density, whereas in the animals treated with the anti-VEGF antibody, there is only slight dilation of the underlying muscle capillaries and some degree of tortuosity.

Figure 4 shows representative histology of DU 145 tumors in animals treated with control antibody 6E10 (Fig. 4A) or A4.6.1 anti-VEGF antibody (Fig. 4B). Sections from control animals showed nodules of poorly differentiated tumor abutting on the deep surface of subcutaneous skeletal muscle. Tumor cells had a high degree of nuclear pleomorphism and abundant eosinophilic cytoplasm. The mitotic indices, expressed as a percentage of the total number of tumor cells, were consistently less than 1%. All but one tumor showed prominent angiogenesis adjacent to and within the tumors (Fig. 4A). Tumors in treated animals were thinner than those in the untreated controls (Fig. 4B). Cytologically, the malignant cells appeared similar to that observed in control animals, with marked nuclear atypia. Mitotic indices were again less than 1%. In two animals, a few capillary vessels were seen adjacent to the tumors, in neither of these were vessels seen within the tumors. No angiogenic response was observed in any of the other animals examined.

Figure 5 (left) shows growth curves in terms of relative tumor area for control animals and treated animals. Since there was no significant difference in growth characteristics between the animals treated with the control antibody as compared with the animals treated with PBS, they were combined in one control group (n = 10). At implantation, the areas of tumors in the control group was 0.37 ± 0.02 mm² and in the treated group 0.37 ± 0.02 mm². Three days after implantation, the areas in the control animals had grown to 1.0 ± 0.07 mm² and in the treated group to 0.97 ± 0.04 mm² ($P$ = 0.6). Seven days after implantation, there was a significant difference in tumor area; 1.12 ± 0.11 mm² in the control group versus 0.92 ± 0.06 mm² ($P$ = 0.02) in the treated group. At the end of the 2-week observation period there was an even more pronounced difference; tumors in the control group had grown to 1.56 ± 0.12, compared with tumors in the treated group, which had grown to only 0.87 ± 0.04 ($P$ < 0.01). Figure 5 (right) shows the angiogenic activity

Mike

**DEPARTMENT OF THE ARMY**
US ARMY MEDICAL RESEARCH AND MATERIEL COMMAND
504 SCOTT STREET
FORT DETRICK, MARYLAND 21702-5012

REPLY TO
ATTENTION OF:

MCMR-RMI-S (70-1y) 26 Nov 02

MEMORANDUM FOR Administrator, Defense Technical Information Center (DTIC-OCA), 8725 John J. Kingman Road, Fort Belvoir, VA 22060-6218

SUBJECT: Request Change in Distribution Statement

1. The U.S. Army Medical Research and Materiel Command has reexamined the need for the limitation assigned to technical reports written for this Command. Request the limited distribution statement for the enclosed accession numbers be changed to "Approved for public release; distribution unlimited." These reports should be released to the National Technical Information Service.

2. Point of contact for this request is Ms. Kristin Morrow at DSN 343-7327 or by e-mail at Kristin.Morrow@det.amedd.army.mil.

FOR THE COMMANDER:

Encl

PHYLLIS M. RINEHART
Deputy Chief of Staff for
Information Management

ADB263708
ADB257291
ADB262612
ADB266082
ADB282187
ADB263424
ADB267958
ADB282194
ADB261109
ADB274630
ADB244697
ADB282244
ADB265964
ADB248605
ADB278762
ADB264450
ADB279621
ADB261475
ADB279568
ADB262568
ADB266387
ADB279633
ADB266646
ADB258871
ADB266038
ADB258945
ADB278624